

# IQARUS

International Workshop on Quantum  
Antimonides Research & Upscaling

# BOOK OF ABSTRACTS



The IQARUS Workshop is funded by the MSCA-ITN - Marie Skłodowska-Curie Innovative Training Networks (ITN) programme: QUANTIMONY: Quantum Semiconductor Technologies exploiting Antimony as part of its dissemination activities.

Quantimony was launched in December 2020 to foster industrial and academic research in the field of antimony-based semiconductor materials. With a duration of 48 months, Quantimony brings together seven universities, one research institute, two large corporations and one SME, enhanced by fourteen partner organizations, to provide high-level training to 14 early-stage researchers in the field of III-Sb semiconductors. The programme covers all aspects of scientific and engineering training from material growth through to industrial exploitation.

# INDEX

<i>PROGRAM SCHEDULE</i> .....	3
<i>SESSION 1</i> .....	4
<i>SESSION 2</i> .....	7
<i>SESSION 3</i> .....	11
<i>SESSION 4</i> .....	16
<i>SESSION 5</i> .....	19
<i>SESSION 6</i> .....	23
<i>SESSION 7</i> .....	28
<i>SESSION 8</i> .....	31
<i>SESSION 9</i> .....	35
<i>POSTER SESSION</i> .....	40

# PROGRAM SCHEDULE



International Workshop on Quantum Antimonides Research & Upscaling

	Monday July 1st	Tuesday July 2nd	Wednesday July 3rd
8:30	Registration		
9:15	Welcome	Registration	Registration
	Session 1 (Alén)	Session 4 (Flatte)	Session 7 (Schineller)
9:30	D.B. CIOMP Changchun (TU Berlin)	Aguado (CSIC)	Weih (Nanoplus GmbH)
10:15	González Posada (U Montpellier)	Candido (U Iowa)	Ramos (IR Nova AB)
11:00	Coffe break		
	Session 2 (Ulloa)	Session 5 (Beanland)	Session 8 (Birner)
11:45	Algora (TU Madrid)	Hakkarinen (U Tampere)	Motyka (U Wroclaw)
12:15	ESR 3 - Schwarz (TU Madrid)	ESR 5 - Acar (U Lancaster)	ESR 12 - Hajrudin (AIXTRON GmbH)
12:45	ESR 4 - Xia (U Lancaster)	ESR 9 - Leguay (TU Berlin)	ESR 10 - Petrovic (U Wuerzburg)
13:15	Lunch catering		
	Session 3 (auf der Maur)	Session 6 (Koenraad)	Session 9 (Llorens)
15:00	Broderick (UC Cork)	Timm (U Lund)	Kesaria (U Cardiff)
15:30	ESR 8 - Zanon (TU Eindhoven)	ESR 6 - Alvarado (U Warwick)	ESR 13 - Sato (nextnano GmbH)
16:00	ESR 14 - Liu (IQE plc)	ESR 7- Trevisan (TU Eindhoven)	ESR 1 - Barbieri (CSIC)
16:30	ESR 11 - Luan (U Tor Vergata)	Fernandez de los Reyes (U Cadiz)	Hartmann (U Wuerzburg)
17:00	Poster session	End	End
17:30	Poster session		
18:30	End		
20:30		Banquet (Salón Elcano - Hotel María Cristina)	

○ Registration 
 ○ Sessions 
 ○ ESR 
 ○ Banquet

More information

[www.iqarus.org](http://www.iqarus.org)



# SESSION 1



# Keynote: Energy efficiency of optical communication in data centers

Dieter Bimberg

*“Bimberg Chinese-German Center for Green Photonics” CIOMP, Chinese Academy of Sciences, Changchun, China and  
Center of Nanophotonics and Institute of Solid State Physics, TU Berlin, Germany*

Since 2018 novel consumer applications like Netflix, Block Chain, LIDAR... and most recently AI not known at that time have led to a huge increase of internet traffic of 60%/year, much more than then originally predicted by companies like Cisco. This increased use of the internet is increasing its electrical power consumption due to increased data traffic mostly inside data centers. New data centers have crossed the 500 MW level. 5G and 6G with their big jumps in data speed will be further enablers for new services, like LIDAR and more, we cannot think about yet, and will increase the energy consumption to an extent not further tolerable.

New device designs are developed by us, focusing on energy-efficiency of data traffic at all hierarchy levels combined with larger data rates. Vertical-cavity surface-emitting lasers (VCSELs) for 200+ Gbit/s single fiber data transmission across OM5 multimode fiber with a record heat to bit rate ratio (HBR) of only 240 fJ/bit x wavelength @ 50Gbit/s developed in our labs are presented [1]. Photon lifetime management is a new key to adopt the overall energy consumption to the bit rate of the data traffic (e.g. 25 Gb/s, 50 Gb/s...) [1].

A completely novel design approach for VCSELs will be presented based on etching multiple holes, oxidizing one or several apertures from these holes and refilling them with metal, in order to increase heat conduction and cut-off frequency and reduce parasitic effects. Thermal roll-over is expected to appear at much larger currents compared to the present standard designs, allowing larger single mode output power and possibly 3-4].

Novel designs of Vertical-Cavity Surface-Emitting Lasers (VCSELs) are presented leading to a strong reduction of thermally induced band gap shift as a function of current and of the series resistance. In our most simple approach (called MUHA 1) blind holes are dry etched into standard devices and then filled with gold resulting in both an effective heat drain technology and electrical shunt, reducing the device series resistance [2]. A different more sophisticated approach (called MUHA 2) uses the dry etched holes to oxidize the apertures [3]. The shape and size of the aperture now depends on the arrangement of holes, opening the way for polarized emission without etching gratings. First results to validate larger output power, rollover current for single mode emission devices, and reduced series resistance are presented for both cases. Finally, multi-aperture VCSELs (called MAVs) based on positioning multiple MUHA 2 in one high power pseudo single-mode emitter are realized [4]

Our new designs are expected to allow for the first time more energy efficient dense wavelength multiplexing across distances of several hundred m to 1 km in data centers.

[1] G. Larisch, R. Rosales, and D. Bimberg, “Energy-efficient VCSELs for 200+ Gb/s optical interconnects”, IEEE J. Select. Topics in Quantum Electronics, 25, 1701105 (2019)

and G. Larisch, S. Tian, D. Bimberg, “Optimization of VCSEL photon lifetime for minimum energy consumption at varying bit rates”, Optics Express 28, 18331 (2020)

[2] M A Maricar, S. Tian, and D. Bimberg, patents in the EU, US and CN, e.g. EP 23199013,

[3] G. Larisch, S. Tian, and D. Bimberg, patents in the EU, US and CN, e.g. EP 3 961 829

[4] G. Larisch, S. Tian, and D. Bimberg, patents the EU, US and CN e.g. EP 4007092

# Keynote: Lasers, photodetectors and sensors based in III-Sb epitaxial materials: Applications exploiting plasmonics

<sup>1\*</sup>Fernando González-Posada Flores

<sup>1</sup> Institute for Electronics and Systems, University of Montpellier, CNRS, 34090 France.

\* [fernando.gonzalez-posada-flores@umontpellier.fr](mailto:fernando.gonzalez-posada-flores@umontpellier.fr)

In the first part of this talk, I will present the Quantum nanostructured components for the mid-infrared (nanoMIR) expertise in III-Sb technology. NanoMIR works with the family of III-V compounds based on GaSb, InAs, AlSb, InSb, their alloys and their heterostructures. In our group, we aim to advance this technology and certain related applications. NanoMIR develops lasers covering the infrared spectral range from 1.5 to 22  $\mu\text{m}$  using different architectures such as quantum cascade lasers, type I quantum well laser diodes and interband cascade lasers. NanoMIR also specializes in infrared photodetectors based on type II superlattices and is developing several gas/molecule detection techniques based on plasmonics and quartz-enhanced photoacoustic spectroscopy.

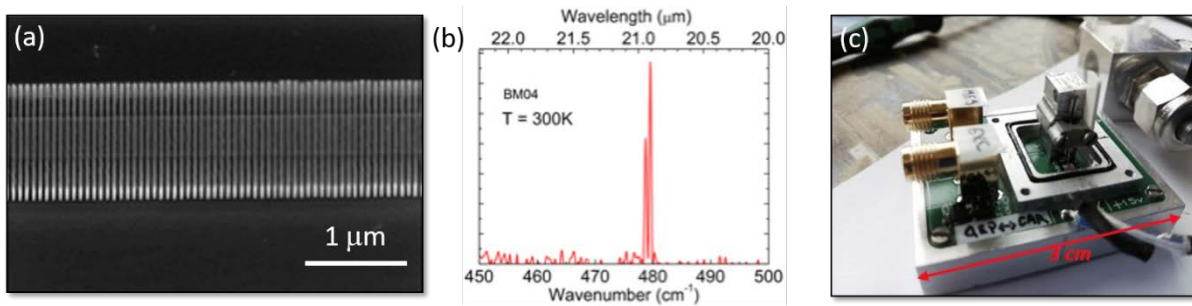


Figure 1(a) SEM Photograph of GaSb-based DFB laser with a lateral metal diffraction grating (b) Emission spectrum of the first semiconductor laser emitting at RT above 20 micrometer (c) Gas sensors based on tunable laser absorption spectroscopy with a compact quartz-enhanced photoacoustic spectroscopy sensor (targeted species:  $\text{CH}_4$ ,  $\text{CO}_2$ ).

In the second part, I will center in application exploiting plasmonics as a very important area of research in nanophotonics. Our approach to plasmonics is made in an original way as we propose to develop metal-free plasmonics. Highly doped semiconductors (HDSCs) can replace current metals such as gold and silver. HDSCs are particularly well suited to mid-IR and THz plasmonics. I will revise the advances of the plasmonics theme developed in the NanoMIR group focusing on three main projects: bio-detection, gas sensing and metamaterials for active plasmonics.

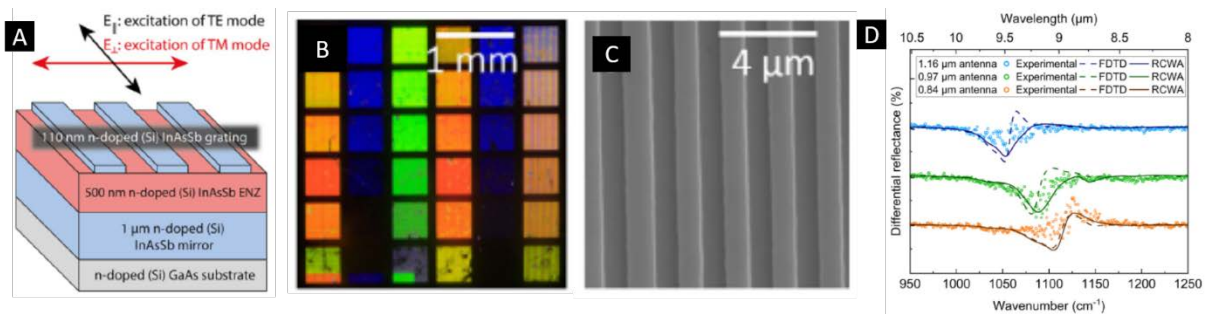


Figure 2. DMMP (Gas sarin) detection with III-V semiconductors: (A) Schematic diagram of the plasmonic sensor. (B) Optical microscopy image of the plasmonic sample displaying different electron beam lithography patterns, each with an area of  $500 \times 500 \mu\text{m}^2$ . (C) Scanning electron microscopy (SEM) image of nano-ribbons antennas. (D) Differential reflectance's ( $\mathcal{E}L$ ): experimental measurements, FDTD simulations and RCWA-corrected simulations.

## SESSION 2



# Invited: Status of III-V flexible solar cells for high power density applications at the Solar Energy Institute of UPM

Carlos Algora\*, Pablo F. Palacios, Daniel Gómez, Clara Sanchez-Perez, Luis Cifuentes, Mercedes Gabás and Iván García  
Instituto de Energía Solar, Universidad Politécnica de Madrid, Spain  
carlos.algora@upm.es

We are developing flexible and lightweight III-V multijunction solar cells for high power density applications such as satellites, unmanned aerial vehicles (drones), High Altitude Pseudo Satellites (HAPS) and high altitude stratospheric balloons for satellite-like communications, cheap and widespread internet connectivity, etc. We focus our research on two different types of III-V solar cells covering the range from 1 kW/kg to 4 kW/kg (considering the weight of the solar cell itself and not that of the module). Our approach to achieve a goal of 4 kW/kg is based on inverted solar multijunction solar cells. We have developed GaInP/GaAs/GaInAs 3J inverted metamorphic solar cells with a power density of 5.7 kW/kg for small areas.

In addition, we are developing lower-cost designs, targeting 1 kW/kg, based on GaInP/Ga(In)As/Ge 3J lattice matched solar cells. In this talk, we present the advances in the modelling, manufacturing and characterization of this last type of solar cell. Modelling shows that solar cell thicknesses of 30 and 60  $\mu\text{m}$  with 20 and 10  $\mu\text{m}$  of Ag rear contact, respectively, require cell efficiencies of 30% to achieve such power densities. Thinner solar cell thicknesses would relax the efficiency target below 30%. Optimizations indicate that 3J solar cells with Distributed Bragg Reflector (DBR) can achieve BOL (Beginning of Life) efficiencies of 31-32% (AM0) for thicknesses ranging 10-100  $\mu\text{m}$  without any additional rear passivation. We have manufactured complete non-thinned (150  $\mu\text{m}$ ) and thinned solar cells (50  $\mu\text{m}$ ) on the same epiwafer to allow a direct comparison. The characterization results confirm our simulations that the efficiency of both cells is the same, enabling a simpler fabrication process without back surface passivation in thinned, flexible solar cells. Experimental power-to-mass densities over 1.2 kW/kg have been preliminary achieved.

# Type-II Super Lattices for Photovoltaics: Analysis of Carrier Collection Efficiency by an Optoelectronic Study as a Function of Temperature

<sup>1,\*</sup>Malte Schwarz, <sup>1</sup>A. Gallego Carro, <sup>1</sup>S. Catalán-Gómez, <sup>2</sup>V. Braza, <sup>2</sup>S. Flores, <sup>2</sup>D. Fernandez-Reyes, <sup>2</sup>T. Ben, <sup>2</sup>D. González, <sup>1</sup>A. Guzman, <sup>1</sup>A. Hierro, <sup>3,4</sup>U. Aeberhard, <sup>1</sup>J.M. Ulloa

\*lead presenter, [malte.schwarz@upm.es](mailto:malte.schwarz@upm.es)

<sup>1</sup>Institute for Optoelectronic Systems and Microtechnology (ISOM), Universidad Politécnica de Madrid, Avda. Complutense 30, 28040 Madrid, Spain

<sup>2</sup>University Research Institute on Electron Microscopy & Materials, (IMEYMAT), Universidad de Cádiz, 11510 Puerto Real, Spain

<sup>3</sup>Fluxim AG, Katharina-Sulzer-Platz, CH-8400 Winterthur, Switzerland

<sup>4</sup>Integrated Systems Laboratory, ETH Zürich Gloriastrasse, Zurich, Switzerland

GaAsSb/GaAsN type-II superlattice (SL) structures are promising metamaterials for the 1eV layer in a multi-junction solar cell. To develop a fundamental understanding of the SL performance and evaluate recombination and transport, an optoelectronic characterization as a function of temperature is performed in this work.

Two solar cells (SCs) of GaAsSb/GaAsN SLs are compared to study the effect of different period thicknesses (SC-SL 3nm, SC-SL 6nm). GaAs and bulk GaAsSbN (SC-bulk) solar cells are included as a reference. Furthermore, samples that underwent rapid thermal annealing cycles (RTA) are also studied. Dark IV curves, solar cell performance under AM1.5G conditions and unintentional doping (UID) are studied as a function of temperature (15K-330K).

By means of drift-diffusion modelling, material parameters such as the Shockley–Read–Hall (SRH) lifetime  $\tau_{SRH}$  and the temperature dependent mobility  $\mu(T)$  are estimated.

In the SLs, the solar cell efficiency peaks between 150K and 200K (Fig. 1), which is related to competing temperature trends in short-circuit current,  $J_{SC}$ , and open-circuit voltage,  $V_{OC}$  (Fig. 2). We attribute a rise in  $V_{OC}$  to reduced recombination and a decline in  $J_{SC}$  to an N-related temperature dependence of mobility. The UID is found to be thermally activated. Samples that underwent RTA retain their superior  $J_{SC}$  over the entire temperature range. This points towards increased mobility, thus, reduced N-related impurity scattering by RTA.

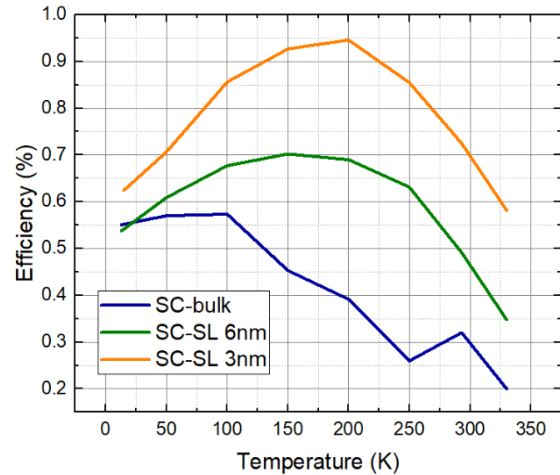


Fig. 1. Solar cell efficiency under AM1.5G conditions

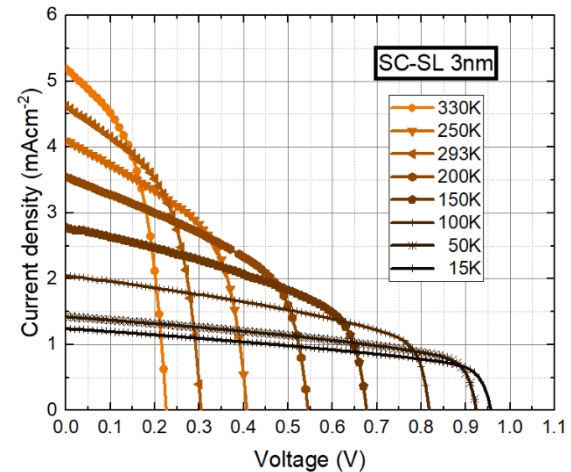


Fig. 2. JV curves of SC-SL 3nm under AM1.5G conditions between 15K and 330K.

# Scaling of ULTRARAM: Fabrication, characterization and simulation of III-V compound-semiconductor non-volatile memory

<sup>1</sup>\*Xiuxin Xia, <sup>1,2</sup>Peter D. Hodgson, <sup>1,2</sup>Manus Hayne.

\*lead presenter

<sup>1</sup>x.xia7@lancaster.ac.uk, Department of Physics, Lancaster University, UK

<sup>2</sup>Quinas Technology Limited, UK

A multiplicity of studies in the last few decades has sought to align the performance of memory with the growing demand from the market. DRAM and flash are prevalent memories, dominating in main memory and mass data storage respectively. Their usage is mainly restricted by their inherent drawbacks. DRAM is a high-speed memory, but is volatile since it's built on a single transistor and capacitor architecture, and requires regular refreshing. In contrast, flash memory, constructed from floating gate metal oxide semiconductor field effect transistors (FGMOSFETs), is capable of holding information without a power supply. However, flash is limited by poor endurance and program/erase speeds as a consequence of utilization of an oxide barrier layer to trap the charge. Therefore, an energy efficient 'universal memory' that offers the speed and endurance of DRAM with the non-volatility of flash has been a considerably sought solution, but was thought impractical due to the counterintuitive properties such as device would require.

Originating from III-V compound semiconductors, **ULTRARAM** is a novel memory exploiting a patented triple-barrier resonant-tunnelling structure (TBRT) that takes advantage of the band offsets between InAs and AlSb. **ULTRARAM** outperforms flash with orders of magnitude lower switching energies [1]. Simulations on the TBRT has indicated its outstanding tolerance to variation in layer thicknesses of growth [2], which is encouraging for imminent production on large wafers. **ULTRARAM** devices with gate dimensions of 10  $\mu\text{m}$  have been grown on Si substrates, fabricated and characterized, demonstrating compatibility with standard semiconductor industry manufacturing [3]. Scaling down to nm dimensions is a critical step on **ULTRARAM**'s miniaturization route towards commercialisation. Here we report the results and analysis of the scaling of single cell **ULTRARAM** devices.

The first attempts at **ULTRARAM** prototype device fabrication used a wet-etch process which is incompatible with scalability. Early attempts at dry-etching produced devices that suffered from channel readout issues caused by the poor conductivity of InAs as a consequence of inevitable channel over-etching. This has been resolved in a newly proposed design with improved device geometry that maintains all merits from legacy fabrication. Cross-sectional studies by electron microscopy have provided the impetus for nextnano simulations [4] of the intermixing and segregation at interfaces of the TBRT heterostructure, complementing earlier work looking at simple changes in TBRT layer thickness [2]. Memory performance metrics such as endurance and retention, as well as simulation and fabrication evolution will be discussed. In this study, we present findings for the fabrication of device at <10  $\mu\text{m}$  gate sizes, a milestone in the miniaturization route towards nm-scale.

**Acknowledgement:** This work is supported by European Union's Horizon 2020 research and innovation programme under the Marie Skłodowska-Curie grant agreement n° 956548, project Quantimony.

[1] Tizno, Ofogh, *et al.* Scientific reports 9.1 (2019): 1-8. [2] Lane, Dominic, and Hayne, Manus, Journal of Physics D: Applied Physics 54.35 (2021): 355104. [3] Hodgson, Peter D., *et al.* Advanced Electronic Materials (2022): 2101103. [4] S. Birner, Website of nextnano GmbH company, available at: <https://www.nextnano.com/>

# SESSION 3



# Invited: Quantitative in silico design of Sb-based quantum-confined heterostructures for optical emission and absorption

Cónal Murphy<sup>1,2</sup>, Eoin P. O'Reilly<sup>1,2</sup> and Christopher A. Broderick<sup>2,1,\*</sup>

<sup>1</sup>Tyndall National Institute, University College Cork, Dyke Parade, Cork T12 R5CP, Ireland

<sup>2</sup>School of Physics, University College Cork, Cork T12 YN60, Ireland

\*Presenting author, email: [christopher.broderick@ucc.ie](mailto:christopher.broderick@ucc.ie)

The broad scope for applications of compact and efficient light emitters and absorbers at mid-infrared wavelengths continues to drive strong research interest in the development of heterostructures based on antimonide III-V semiconductors. In this talk we will review three recently-explored classes of such heterostructures from a theoretical perspective.

First, we describe the electronic and optical properties of metamorphic  $\text{InAs}_{1-x}\text{Sb}_x/\text{Al}_y\text{In}_{1-y}\text{As}$  quantum well (QW) LEDs grown on GaAs substrates using a relaxed  $\text{Al}_y\text{In}_{1-y}\text{As}$  metamorphic buffer layer (MBL) [1]. Exploiting lattice engineering via the MBL composition allows to grow compressively strained QWs possessing tuneable type-I band offsets, and hence to extend the benefits of strained QWs to the mid-infrared. Theory-experiment comparisons highlight the ability to increase the radiative recombination rate by increasing the Sb composition in the QW, while activation energy (Arrhenius) fitting indicates that the ability to engineer a large conduction band offset allows to mitigate thermal leakage of electrons.

Second, we extend our multi-band  $\mathbf{k}\cdot\mathbf{p}$  calculations for QWs to treat superlattices (SLs). Utilising the natural periodicity associated with a plane wave basis set, we demonstrate numerically efficient computation of SL electronic structure – incl. miniband dispersion – utilising a calculational supercell consisting of a single SL period. Using the  $\mathbf{k}$ -dependent SL eigenstates as input, and explicitly accounting for minibands, we compute spontaneous emission spectra and the radiative recombination rate. Selecting InAs/GaSb as an exemplar broken-gap SL system, we (i) quantify the impact of miniband formation on radiative recombination, and (ii) perform high-throughput calculations to maximise the room-temperature radiative recombination coefficient  $B$  across the 3.5 – 7  $\mu\text{m}$  wavelength range [2].

Third, we apply our multi-band  $\mathbf{k}\cdot\mathbf{p}$  simulation framework to type-II InAs/InAs<sub>1-x</sub>Sb<sub>x</sub> SLs grown on GaSb substrates. When grown on [001] GaSb, InAs is tensile-strained. Varying the Sb composition, in addition to the InAs and InAs<sub>1-x</sub>Sb<sub>x</sub> layer thicknesses, then allows to design strain-balanced type-II SL structures [3]. This effectively results in two endpoint design regimes: (i) thick layers with low Sb composition, or (ii) thin layers with high Sb composition. We systematically vary the layer composition and thickness and, again using the  $\mathbf{k}$ -dependent SL eigenstates as input, compute the optical absorption. We optimise these SLs for photodetector applications by maximising optical absorption at wavelengths close to 5  $\mu\text{m}$ .

[1] E. Repiso, C. A. Broderick, M. de la Mata, R. Arkani, Q. Lu, A. R. J. Marshall, S. I. Molina et al., *J. Phys. D: Appl. Phys.* **52**, 465102 (2019)

[2] C. Murphy, E. P. O'Reilly and C. A. Broderick, *J. Phys. D: Appl. Phys.* **57**, 035103 (2024)

[3] C. A. Broderick, S. Jin, I. P. Marko, K. Hild, P. Ludewig, Z. L. Bushell, W. Stolz, J. M. Rorison, E. P. O'Reilly, K. Volz and S. J. Sweeney, *Sci. Rep.* **7**, 46371 (2017)

# Core-hole manganese spin in III-V semiconductors with a quantum-mechanical treatment

<sup>1\*</sup>Zanon, J., <sup>2, 1</sup> Flatté, M.E.

\*lead presenter

<sup>1</sup>j.zanon@tue.nl, Department of Applied Physics and Science Education, Eindhoven University of Technology, Eindhoven 5612 AZ, The Netherlands

<sup>2</sup>Department of Physics and Astronomy, University of Iowa, Iowa City, Iowa 52242, USA

The control of spin-degree of freedom for applications in sensing and quantum devices has been one of the major goals in semiconductor physics in the past few decades. In III-V semiconductors (e.g., in GaAs or InSb) this could be achieved with manganese impurities. Manganese forms a complex, where a  $J = 3/2$  hole from the host aligns antiferromagnetically with the  $5/2$  spin of the  $3d5$  manganese core, forming a core-hole complex with a total spin  $F = S + J = 1$  [1]. With a classical treatment for the Mn core, theoretical calculations with STM images showed the potential to characterize the spatial structure of a single manganese [2] and the exchange interaction between manganese pairs [3]. Still in this classical treatment, calculations pointed out that changing the spin orientation from the core would affect the spatial structure of the manganese complex [4]. In our work, based on previous ESR measurements [1], we show a new pathway to treat the manganese core fully quantum-mechanically. Using an effective mass approximation to treat the hole part of the wavefunction [2], we demonstrated analytically that the spatial structure of a single manganese in bulk III-V semiconductors depends on the x-component of the spin texture produced by the total spin  $F$ .

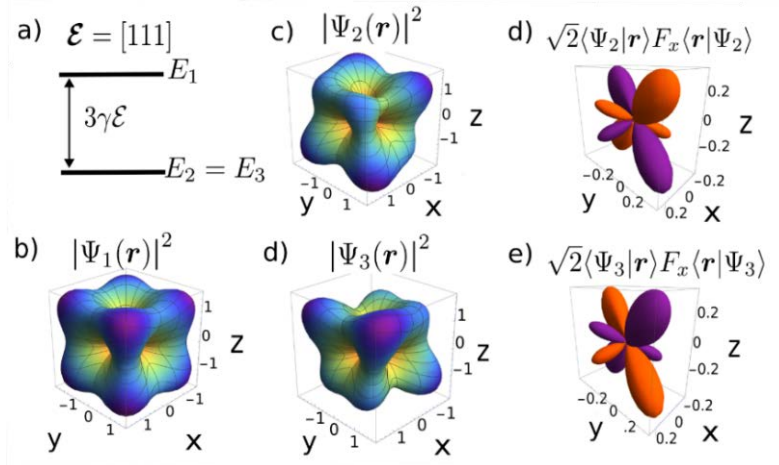


Figure 1. An external electric field  $\boldsymbol{\varepsilon}$  along the  $[111]$  direction splits the energy  $E_{F=1}$  in a) leaving two states degenerate. b), c) and d) show how each state has a different spatial structure. The cubic shape changes due a non-zero spin texture in d) and e).

[1] J. Schneider, U. Kaufmann, W. Wilkening, et al., Phys. Rev. Lett. 59, 240 (1997).

[2] A. M. Yakunin, A. Y. Silov, P. M. Koenraad, et al., Phys. Rev. Lett. 92, 216806 (2004)

[3] D. Kitchen, A. Richardella, J.-M. Tang, et al., Nature 442, 436 (2006).

[4] Jian-Ming Tang, Jeremy Levy, and Michael E. Flatté. Phys. Rev. Lett. 97, 106803 (2006).

This project has received funding from the European Union's Horizon 2020 research and innovation programme under the MarieSkłodowska-Curie grant agreement No 956548.

# Growth of InAs/GaSb Type-II superlattices by Metalorganic Chemical Vapor Deposition

Chen Liu<sup>1,2\*</sup>, Loganathan Ravi<sup>2</sup>, Manoj Kesaria<sup>1</sup>, Iwan Davies<sup>2</sup>

\*Email: [chenliu@iqep.com](mailto:chenliu@iqep.com)

<sup>1</sup>School of Physics and Astronomy, Cardiff University, United Kingdom

<sup>2</sup>IQE plc, Cardiff, Wales, CF3 0LW, United Kingdom

Mid-wave and long-wave infrared detectors are crucial in various applications, including night vision, motion detection, and thermal imaging [1]. InAs/GaSb Type-II superlattices (T2SLs) have emerged as promising alternatives to HgCdTe for infrared detectors [2] due to their flexible band gap engineering and advantageous manufacturability. Despite excellent achievements in experiments by molecular beam epitaxy (MBE) [3], reports about the growth by metalorganic chemical vapor deposition (MOCVD) are limited and problematic due to strained interfaces [4]. Here we present the growth of InAs/GaSb T2SLs on InAs and GaSb substrates using MOCVD. Lattice-matched T2SLs were obtained on InAs substrates with excellent surface morphology.

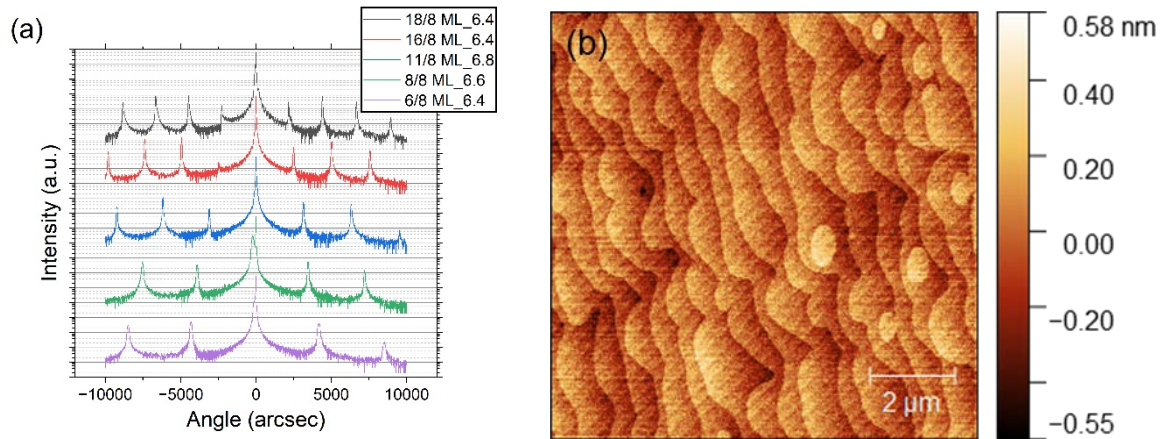


Fig.1 (a)  $\omega$ - $2\theta$  scans for different InAs/GaSb T2SLs with different structure on InAs wafers. (b) Atomic force microscope (AFM) image ( $8 \times 8 \mu\text{m}$ ) for 16/8 ML InAs/GaSb T2SL on an InAs wafer. The root mean square (RMS) is 0.14 nm.

**References:** [1] F. Zhuge et al., Adv. Mater. Technol. 2, 1700005 (2017). [2] A. Rogalski, Infrared Phys. Technol. 54, 136-1545 (2011). [3] D. C. M. Kwan et al., Appl. Phys. Lett. 118, 203102 (2021). [4] X. B. Zhang et al., J. Cryst. Growth 287, 545-549 (2006).

# Empirical Tight-Binding simulations for disordered semiconductor alloys

<sup>1</sup>\*Phan, A.-L., <sup>2</sup>Pecchia, A., <sup>1</sup>Di Vito, A., <sup>1</sup>Soccodato, D. & <sup>1</sup>Auf der Maur, M.  
\*lead presenter

<sup>1</sup> anh.luan.phan@uniroma2.it, University of Rome “Tor Vergata”, Italy

<sup>2</sup> ISMN-CNR, Italy

The alloy disorder is of crucial importance in optoelectronic devices involving alloyed materials. On the other hand, the alloy-like configurations can be present unintentionally in cases of hetero-interfaces due to atomic inter-diffusion, intermixing and segregation. In such alloyed materials and alloy-like configurations, the chemical species and the strain profiles are irregular and complicated. Moreover, in practice the alloy concentration may be non-uniform across the whole system, which adds even more complexities. Therefore, understanding the impacts of the alloy disorder on electronic and optical properties is important. This raises the need of theoretical models to incorporate the alloy disorder's effects into calculations of the electronic and optical properties of the materials/devices. In this context, an atomistic theory like density functional theory (DFT) is preferable, but the expensive computational cost of DFT limits its applicability since the random alloy simulations require large supercells and many structure configurations. As an alternative, the empirical tight-binding (ETB) method, which is also an atomistic model, can well balance between the computational demand and the required accuracy.

Of the various ETB schemes ever proposed, one of the most widely used schemes for group-IV and III-VI semiconductors is that of Jancu et al. [1]. However, Jancu's scheme and its variants/modifications are limited in treating strain effects in random alloys due to lacking of important corrections accounting for the changes in the local environment surrounding each ion compared to that in the bulk cases. Consequently, Jancu's scheme fails to reproduce the band gaps' variations of some important III-V alloys such as GaAsSb and InAsSb. We discuss two approaches in the framework of ETB that can resolve this limitation. The first one employs the power of Machine Learning (ML) to add the proper corrections to the onsite energies for each ion by learning from reference DFT targets. This ML-based approach turns out to be able to work very well for Jancu's scheme without introducing extra parameters to the ETB model. On the other hand, a physics-based approach backed by a recently proposed scheme of Tan et al. [2] addresses the limitation of Jancu's scheme by adding parameters accounting for the corrections from the multipole expansion analysis of the atomic potentials to both onsite and hopping energies. This new scheme in fact can also give alloys' band gaps aligned excellently with the experimental data. We will analyze the pros and cons of each approach and then demonstrate a practical application of ETB in large-supercell simulations for a typical disordered semiconductor alloy GaAsSb as an example. The results will be shown to be in good agreement with the experimental observations, which is a proof for the efficacy of the ETB method in investigating disordered alloyed structures.

[1] J.-M. Jancu, R. Scholz, F. Beltram, and F. Bassani, “Empirical spds\* tight-binding calculation for cubic semiconductors: General method and material parameters,” *Phys. Rev. B*, vol. 57, pp. 6493–6507 (1998).

[2] Y. Tan, M. Povolotskyi, T. Kubis, T. B. Boykin, and G. Klimeck, “Transferable tight-binding model for strained group IV and III-V materials and heterostructures,” *Phys. Rev. B*, vol. 94, p. 045311 (2016).

# SESSION 4



# Keynote: From Majorana to Andreev and back.

Ramón Aguado

Instituto de Ciencia de Materiales de Madrid (ICMM - CSIC), Madrid, Spain  
raguado@icmm.csic.es

The interplay of spin-orbit coupling, Zeeman fields and low densities in semiconducting devices (InAs, InSb) proximitized by superconductors can induce a quantum phase transition into a topological superconducting phase with Majorana zero modes (MZMs). Quite remarkably, MZMs do not follow fermion statistics, unlike the original particles predicted by Majorana, but rather possess non-Abelian exchange statistics. This property, together with their topological protection against local noise, holds promise for applications in fault-tolerant topological quantum computing [1]. However, after more than ten years of intense experimental effort towards the unambiguous detection of Majoranas, it has become evident that distinguishing them from subgap Andreev bound states (ABS)s near zero energy, which are ubiquitous in such hybrid semiconductor-superconductor devices due to various physical mechanisms, is extremely difficult. Interestingly, this Majorana versus Andreev controversy [2] has helped us to understand that, far from being a disadvantage, the presence of ABSs can be used to design new qubit concepts. One promising route is to encode a qubit in the spin of a quasiparticle occupying an ABS in a quantum dot-based Josephson junction [3,4]. Embedding such superconducting spin qubit in a superconducting transmon circuit, allows an intrinsic spin-supercurrent coupling providing an optimal interface with circuit quantum electrodynamics for coherent control, readout and strong coherent qubit-qubit coupling [5]. By extending this idea to Josephson junctions based on a minimal chain of four quantum dots one could demonstrate a minimal Majorana-Transmon qubit based on non-local fermion parity [6].

[1] *Majorana qubits for topological quantum computing*, Ramón Aguado, Leo P Kouwenhoven, *Physics Today* 73 (6), 44-50 (2020).

[2] *From Andreev to Majorana bound states in hybrid superconductor-semiconductor nanowires*, Elsa Prada, Pablo San-Jose, Michiel WA de Moor, Attila Geresdi, Eduardo JH Lee, Jelena Klinovaja, Daniel Loss, Jesper Nygård, Ramón Aguado, Leo P Kouwenhoven, *Nature Review Physics*, 2, 575–594 (2020).  
pages 575–594 (2020)

[3] *Singlet-Doublet Transitions of a Quantum Dot Josephson Junction Detected in a Transmon Circuit*, Arno Bargerbos, Marta Pita-Vidal, Rok Žitko, Jesús Ávila, Lukas J. Splitthoff, Lukas Grünhaupt, Jaap J. Westorp, Christian K. Andersen, Yu Liu, Leo P. Kouwenhoven, Ramón Aguado, Angela Kou, and Bernard van Heck, *PRX Quantum* 3, 030311 (2022).

[4] *Spectroscopy of Spin-Split Andreev Levels in a Quantum Dot with Superconducting Leads*, Arno Bargerbos, Marta Pita-Vidal, Rok Žitko, Lukas J. Splitthoff, Lukas Grünhaupt, Jaap J. Westorp, Yu Liu, Leo P. Kouwenhoven, Ramón Aguado, Christian Kraglund Andersen, Angela Kou, and Bernard van Heck, *Phys. Rev. Lett.* 131, 097001 (2023)

[5] *Direct manipulation of a superconducting spin qubit strongly coupled to a transmon qubit*, Marta Pita-Vidal, Arno Bargerbos, Rok Žitko, Lukas J Splitthoff, Lukas Grünhaupt, Jaap J Westorp, Yu Liu, Leo P Kouwenhoven, Ramón Aguado, Bernard van Heck, Angela Kou, Christian Kraglund Andersen, *Nature Physics*, 19, 1110 (2023)

**pages**

[6] *Minimal Kitaev-transmon qubit based on double quantum dots*, D Michel Pino, Rubén Seoane Souto, Ramón Aguado, *Phys. Rev. B*, 109, 075101 (2024)

# Keynote: Quantum oscillations as a tool for unraveling band structures

<sup>1</sup>\*Candido, D.R..

<sup>1</sup>[denis-candido@uiowa.edu](mailto:denis-candido@uiowa.edu), Department of Physics and Astronomy, University of Iowa, USA.

Shubnikov-de Haas (SdH) oscillations – or quantum oscillations – have served as a paradigmatic experimental probe and tool for extracting key semiconductor parameters such as carrier density, effective mass, Zeeman splitting with  $g$  factor  $g^*$ , quantum scattering time, and Rashba  $\alpha$  and Dresselhaus  $\beta$  spin-orbit (SO) coupling parameters. Analytical descriptions of the SdH oscillations are available for some special cases, but no analytical solution could be found for the vast majority of parameter space with all three terms present. Despite over 50 years of experiments and many theoretical models, which were put forth, this has seriously hampered the analysis and interpretation of experimental data. Here, we bridge this gap by providing an analytical formulation for the SdH oscillations of 2D electron gases (2DEGs) with simultaneous Rashba, Dresselhaus, and Zeeman interactions over a very broad range of parameter space [1]. More importantly, we derive a simple condition for beating-free SdH oscillations for all harmonics in 2DEGs in the presence of both Rashba, Dresselhaus and Zeeman interaction [1]. For the conditions in which analytical results are not possible to be obtained, we have developed a numerical method for studying SdH oscillations in the presence of both Rashba, Dresselhaus and Zeeman interaction, and also for an in-plane component of the magnetic field [2].

Furthermore, we demonstrate that when the non-trivial topology of a semiconductor electronic system is produced by inverted bands with “Mexican-hat” shape, SdH oscillations show an anomalous beating pattern that is solely due to the non-trivial topology of the system [3]. These beatings are distinct from beatings originating from spin-orbit interactions, and provide a direct way to experimentally probe the non-trivial topology of 2D TIs entirely from a bulk measurement. Furthermore, the Fourier transform of the SdH oscillations as a function of the Fermi energy and quantum capacitance models allows for extracting both the topological gap and gap at zero momentum [3].

Finally, we also discuss SdH oscillations in 2DEG of complex oxides, EuO/KTaO (EuO/KTO) and LaAlO/SrTiO (LAO/STO). To accurately resolve these oscillations, we conducted transport measurements in high magnetic fields up to 60 T and low temperatures down to 100 mK [4]. For 2D confined electrons at both interfaces, we observed a progressive increase of oscillations frequency and cyclotron mass with the magnetic field. We interpret these intriguing findings due to the large effective mass and large Rashba spin-orbit coupling.

[1] DR Candido, SI Erlingsson, H Gramizadeh, JVI Costa, PJ Weigele, DM Zumbühl, JC Egues, PRR 5, 043297 (2023).

[2] H Gramizadeh, DR Candido, A Manolescu, JC Egues, SI Erlingsson, PRB 109, 115303 (2024).

[3] DR Candido, SI Erlingsson, JVI Costa, and JC Egues, arXiv:2406.08977

[4] Km Rubi, DR Candido, et., al.,, arXiv:2307.04854

# SESSION 5



# Invited: Telecom wavelength non-classical light sources based on GaSb quantum dots grown by filling droplet-etched nanoholes

Teemu Hakkarainen

Institute of Advanced Study, University of Tampere (Finland)

teemu.hakkarainen@tuni.fi

## Abstract:

Solid-state single and entangled photon emitters linked coherently over long distances with optical fibers enable a new generation of quantum-based communications networks. Currently, epitaxial semiconductor quantum dots (QDs) pave the way as a scalable approach for fabricating deterministic non-classical light sources that can be integrated with other photonic or electronic components in miniaturized form. Here, we present a new quantum material system based on GaSb QDs formed by filling droplet-etched nanoholes [1,2], a technique which has been previously used for the state-of-the-art single- and entangled-photon sources in the GaAs-based materials emitting at wavelengths shorter than 800 nm [3-6]. We show that while the GaSb QDs exhibit high homogeneity and small fine structure splitting similarly to their GaAs counterparts, they also enable single-photon emission in the 3rd telecom window [7] with prospects for extending towards 2 $\mu$ m. These properties make them ideal candidates for quantum photonic applications requiring compatibility with Si-photonics and fiber-based telecom.

[1] J. Hilska et al. Cryst. Growth Des. 21 1917–1923, 2021

[2] A. Chellu et al. APL Materials 9, pp. 051116, 2021

[3] J. Liu et al. Nature Nanotechnology 14, 586 (2019).

[4] D. Huber et al. Nature Communications 8, 15506 (2017).

[5] E. Schoöll, et al. Nano Letters 19, 2404 (2019).

[6] D. Huber et al. Phys. Rev. Lett. 121, 033902 (2018).

[7] J. Michl et al, Adv Quantum Technol. 6, 2300180 (2023).

# Enhancing Quantum Photonics: Novel Single Photon LEDs Utilizing GaSb Quantum Rings at Telecoms Wavelength

<sup>1\*</sup>Acar, G., <sup>1</sup>Hodgson, P., <sup>2</sup>Leguay, L., <sup>1</sup>Jones, S., <sup>2</sup>Schliwa, A., <sup>1</sup>Hayne, M.

<sup>1</sup>Department of Physics, Lancaster University, Lancaster LA1 4YB, UK

<sup>2</sup> Institute of Solid-State Physics, Technical University of Berlin, Berlin 10623, Germany

\*corresponding author: [g.acar@lancaster.ac.uk](mailto:g.acar@lancaster.ac.uk)

In the evolving landscape of quantum technology, single-photon emitters leveraging quantum dots (QDs) present groundbreaking potential in revolutionizing communication and computational systems. The effective deployment of quantum communication systems crucially depends on the availability of efficient, electrically-driven single-photon sources that operate reliably at room temperature and align with the telecommunications spectrum ranging from 1260 to 1675 nm [1]. The proposed SPLEDs utilize type-II GaSb QRs, which are known for their reduced strain and defect rates due to a minimized lattice mismatch when grown via molecular beam epitaxy on GaAs substrates [3,4]. This structural choice not only enhances the efficiency and operational stability of the emitters but also enables emission across a wide wavelength spectrum, critical for integration into existing fiber optic networks.

Our proposed SPLED architecture incorporates a unique electron-filtering layer consisting of non-uniform gallium arsenide (GaAs) QDs embedded in aluminum gallium arsenide (Al<sub>x</sub>Ga<sub>1-x</sub>As) [5]. This configuration not only promotes selective electron injection into multiple QRs but also enhances photon emission efficiency through an engineered optical cavity with distributed Bragg reflectors. Significantly, our empirical research shows that the photon emission qualities of the SPLED remain stable and improve with higher operational temperatures (fig.1) and reduced current values. This represents a notable departure from traditional photonics behavior. The integration of these technologies into a single device offers a groundbreaking approach to photon source design—simplifying manufacturing processes, reducing costs, and improving device robustness and performance under varied environmental conditions. These enhancements make our SPLEDs exceptionally suitable for broad deployment in quantum technologies, potentially revolutionizing quantum key distribution and secure communication channels.

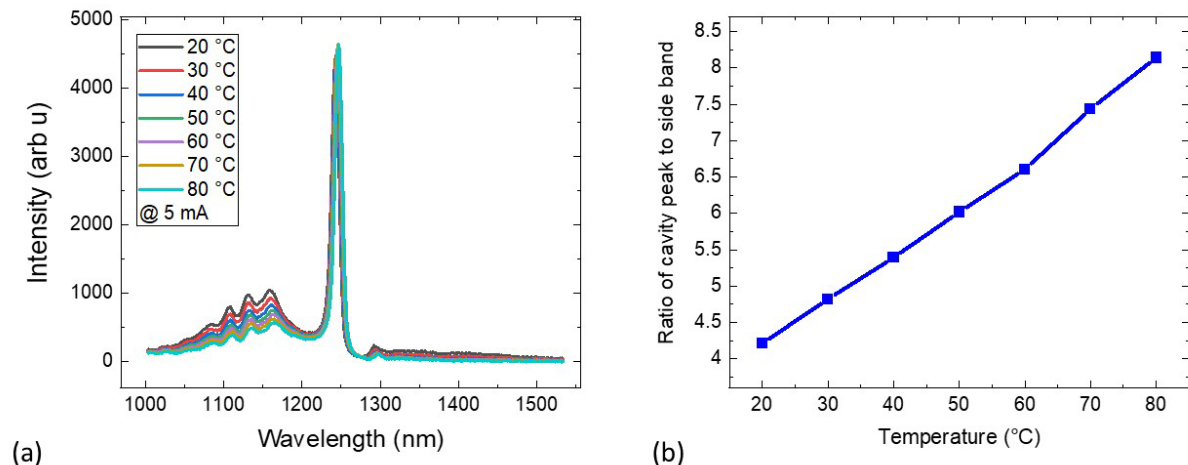


Fig. 1. (a) Electroluminescence intensity vs wavelength from 20 °C to 80 °C under a condition of constant current. (b) Ratio of the cavity peak to side band with elevating temperature.

Acknowledgement: This work is supported by European Union's Horizon 2020 research and innovation programme under the Marie Skłodowska-Curie grant agreement n° 956548, project Quantimomy.

[1] G. Moody *et al.* J. Phys. Photonics, 4 012501 (2022). [3] P. D. Hodgson *et al.*, Applied Physics Letter, **105**, 8 (2014). [4] D. Hodgson *et al.*, Journal of Applied Physics, **119**, 4 (2016).

[5] M. Hayne *et al.* Single photon source. WO2018162894A1 (2018).

# Optimization of semiconductor devices using evolutionary algorithms and nextnano++

<sup>1\*</sup>L. Leguay, <sup>2</sup>H.S. Mączko, <sup>1</sup>A. Schliwa, <sup>2</sup>S. Birner

<sup>1\*</sup>[l.leguay@tu-berlin.de](mailto:l.leguay@tu-berlin.de), Institute of Solid-State Physics, TU Berlin, Germany

<sup>2</sup>nextnano GmbH, Munich, Germany

The vast potential of III-Sb semiconductor materials for diverse nanostructure configurations offers numerous applications in solar cells, lasers, infra-red detectors, and quantum light sources. However, the immense parameter space, including size, shape, chemical composition, and growth axis, remains largely unexplored. This study employs evolutionary algorithms<sup>1,2</sup> to systematically identify optimal designs for specific target properties using an inverse design approach. The developed framework interfaces with the Python module of the nextnano software<sup>3</sup>, enabling comprehensive scanning of the configuration space to identify superior nanostructure designs.

In this presentation, we explore both the optimization of a nitride-based UV LED device, focusing on enhancing its internal quantum efficiency, and a Sb-based infrared detector, targeting improvements in detection efficiency and specificity. Our work also includes optimizing simulation parameters for diverse Sb-based devices to ensure convergence and accuracy, facilitating reliable device simulations.

This study highlights the potential of evolutionary algorithms in advancing semiconductor technology, showcasing their application in III-Sb heterostructures and nitride-based UV LEDs. Our results underscore the necessity for continued research and the development of robust computational tools to unlock the full potential of these materials.

<sup>1</sup>H. G. Beyer and H. P. Schwefel, *Natural Computing* 1(1):3-52 (2002).

<sup>2</sup>N. Hansen et al, *Springer Handbook of Computational Intelligence* Pages 871–898 (2015).

<sup>3</sup>S. Birner et al, *IEEE Trans. Electron. Devices* 54 2137 (2007).

# SESSION 6



# Invited: Atomic-scale surface properties of III-V semiconductor nanostructures

Rainer Timm

[Rainer.timm@sljus.lu.se](mailto:Rainer.timm@sljus.lu.se), NanoLund and Department of Physics, Lund University, Sweden

III-V semiconductor nanostructures, with their superior charge carrier mobility and a direct and tunable band gap, are promising for next generation devices in electronics, photonics, energy harvesting, and quantum information. With the decreasing size of structures and devices increases the relevance of the surface for novel physical effects and for dominating device performance. Here, I will present our toolbox for the atomically resolved surface characterization and modification of semiconductor nanostructures, based on scanning tunnelling microscopy and spectroscopy (STM/S) as well as synchrotron-based X-ray photoelectron spectroscopy (XPS) in various setups.

In the first part of my presentation, I will focus on III-V semiconductor nanowires, i.e. crystalline rods with about 20 – 200 nm diameter and up to several  $\mu\text{m}$  length. Nanowires of different III-V alloys can easily be stacked on top of each other, and they can epitaxially be grown on silicon without interfacial defects due to their small footprint, combining III-V functionality with the established silicon technology platform. We map nanowires across axial heterostructures between different materials [1], doping level [2], or different crystal phase [3,4], where we correlate the surface structure and local electronic properties, down to quantum size effects [4]. Of special interest are *operando* experiments during nanowire device operation [2] and *in-situ* studies upon surface modification [5,6]. Nanowire crystal phase heterostructures can act as templates for radial overgrowth with atomic-scale control, monitored by STM: Figure 1 shows the surface of a GaAs nanowire which has been exposed to Bi atoms, resulting in the self-selective formation of well-ordered GaBi 1D and 2D nanostructures on the surface of the wurtzite segment, while only individual Bi atoms or small Bi clusters were incorporated in the zincblende surface [6].

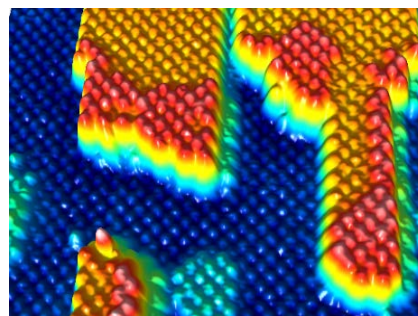


Figure 1: **STM image of GaBi islands on the [11-20] surface of a wurtzite GaAs nanowire [6].**

In the second part, I will show some recent results of Bi deposition on InSb surfaces. This material combination is characterized by very large spin-orbit splitting, promising for spintronic and quantum applications. We observe different types of Bi-induced surface structures on InSb(110) and (111)A/B as well as different bonding environments, including In-Bi, Sb-Bi, and Bi-Bi bonds. Density functional theory models of the observed Bi-induced surfaces on both GaAs [7] and InSb predict nontrivial topological behavior, which is supported by initial STS and angle-resolved photoelectron spectroscopy measurements.

## References:

- [1] Liu et al., Appl. Phys. Lett. 117 (2020) 163101.
- [2] McKibbin et al., Nano Lett. 20 (2020) 887.
- [3] M. Hjort et al., Nano Lett. 13 (2013) 4492.
- [4] J. Knutsson et al., ACS Nano 11 (2017) 10519.
- [5] Liu et al., Appl. Surf. Sci. 593 (2022) 153336.
- [6] Liu et al., Nature Commun. 12 (2021) 5990.
- [7] Liu et al., ACS Nano 17 (2023), 5047.

# Quantification of antimony in ultra-thin InAs/AlSb layers using energy dispersive x-rays (EDX) and multislice simulations

<sup>1\*</sup>Francisco Alvarado-Cesar, <sup>2</sup>Peter Hodgson, <sup>2</sup>Manus Hayne, <sup>3</sup>Verónica Braza, <sup>3</sup>Daniel F. Reyes, <sup>3</sup>Teresa Ben, <sup>3</sup>David González & <sup>1</sup>Richard Beanland.

\*lead presenter

<sup>1</sup>Francisco.Alvarado-Cesar@warwick.ac.uk, University of Warwick, United Kingdom

<sup>2</sup>Lancaster University, United Kingdom

<sup>3</sup>Universidad de Cádiz, Spain

ULTRARAM is a low-voltage, ultrafast, non-volatile memory growth by molecular beam epitaxy (MBE) that instead of using the a SiO<sub>2</sub> barrier to access to the floating gate memory, is accessed through a triple barrier made by InAs/AlSb heterostructure of only a few nanometer in thickness [1]. However, antimony (Sb) tends to segregate over long distances, resulting in a notable variation of composition across the interfaces and the formation of the quaternary compound  $Al_xIn_{1-x}As_ySb_{1-y}$ . Consequently, the specifics of how composition changes at this interface remain ambiguous and require further studies.

Annular dark-field scanning transmission electron microscopy (ADF-STEM) is an excellent tool for this analysis, as it allows the differentiation between the atoms from group III (Al,In) and group V (As, Sb), as illustrated in Fig 1 (a). While ADF-STEM provides readily interpretable images and can highlight features like interface roughness, it primarily offers qualitative data. To derive quantitative insights additional methods are required [2]. In this study, we use EDX to know the distribution of the composition through the structure in combination with multislice simulations to obtain quantitative compositional measurements.

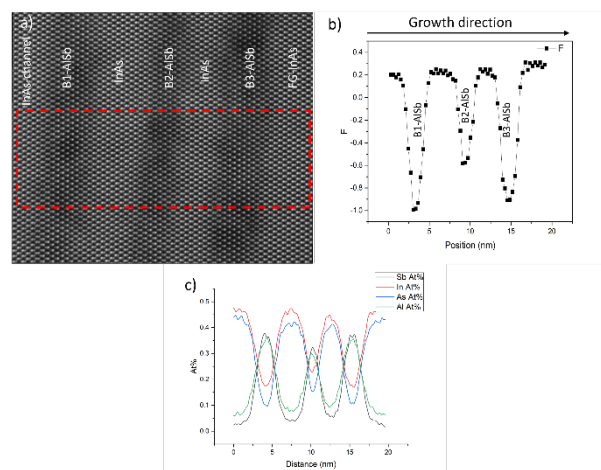


Fig. 1 a) ADF-STEM of InAs:AlSb:InAs:AlSb:InAs:AlSb triple barrier resonant tunneling structure in an ULTRARAM device. Each dumbbell consists of a group III atom column (lower) and group V atom column (upper). b) Intensity form the factor  $F = \frac{I_{III} - I_V}{I_{III} + I_V}$  of the structure c) EDX spectra of the TBRT.

- [1] "Adv Elect Materials - 2022 - Hodgson - ULTRARAM A Low-Energy High-Endurance Compound-Semiconductor Memory on Silicon.pdf."
- [2] D. Gonzalez *et al.*, "Identification of the Segregation Kinetics of Ultrathin GaAsSb/GaAs Films Using AlAs Markers," *Nanomaterials*, vol. 13, no. 5, p. 798, Feb. 2023, doi: 10.3390/nano13050798.

# Cross-sectional scanning tunneling microscopy characterization of III-V Sb-based materials

<sup>1\*</sup>Trevisan A., <sup>2</sup>Hodgson P. D., <sup>3</sup>Lane D., <sup>4</sup>Gallego Carro A., <sup>4</sup>Ulloa J. M.,  
<sup>2</sup>Hayne M. & <sup>1</sup>Koenraad P. M.

\*lead presenter

<sup>1</sup>a.trevisan@tue.nl, Department of Applied Physics and Science Educations, Eindhoven University of Technology, Eindhoven, The Netherlands

<sup>2</sup>Department of Physics, Lancaster University, Lancaster, United Kingdom

<sup>3</sup>The School of Electrical and Mechanical Engineering, University of Adelaide, Adelaide, South Australia, Australia

<sup>4</sup>Institute for Optoelectronic Systems and Microtechnology, Universidad Politécnica de Madrid, Madrid, Spain

III-Sb semiconductors have been attracting interest for their potential applications in various devices, for instance memory technologies, solar cells, single photon sources and light emitting diodes (LED) and lasers. This is related to their distinctive physical properties, such as a small effective mass of the carriers and the possibility to tune their band gap from the near-IR to the far-IR wavelength. The performances of these devices strongly depend on the quality of the grown materials, namely sharp interfaces, absence of defects such as stacking faults and dislocation and homogeneous incorporation of dopants. The structural and electronic properties (i.e. interface quality, composition and presence of defects) of semiconductor materials can be studied at the atomic scale by cross-sectional scanning tunneling microscopy (X-STM).

We studied different III-V Sb-based materials and their electronic and structural properties by X-STM. In particular we studied a ULTRARAM sample, a novel non-volatile memory technology based on InAs/AlSb heterostructures (**S1**), GaAsN/GaAsSb superlattices (SLs) for solar cells application (**S2**), GaSb quantum rings (QRs) for LED application (**S3**) and a GaAs<sub>1-x</sub>Sb<sub>x</sub> (0.001 < x < 0.07) multi-layer structure (**S4**). Interface quality and layer thickness were probed in S1 and S2. Moreover, the GaSb QRs' morphology (**S3**) and the behaviour of Sb as iso-electronic dopant in GaAs (**S4**) and its incorporation and segregation were studied.

The formation of stacking faults and AlSb accumulation or nanoridges (NRs) was observed in **S1**, resulting in layers of uneven thicknesses. Differently, the different layers in the SLs sample **S2** have the intended thickness and sharp interfaces. Sb and N concentration of the different layers of the SLs was calculated and compared to the nominal one. The experimental Sb and N concentrations are found to be respectively higher and lower than the nominal one.

In **S3**, three layers of GaSb QRs are imaged. We observed that the QRs do not preferentially form in one of the GaSb layers. The studied QRs show different shapes depending on where they are cleaved. To determine the shape of the QRs, their base length, apparent diameter and height and shape of the ring body were measured.

In **S4**, Sb atoms up to four layers below the surface are visible in the X-STM images and are in classified and related to their depth below the cleavage surface. Sb incorporation and segregation are studied for the layers at lower Sb content using Muraki's model. Under the applied growth condition, Sb is readily incorporated in GaAs and show a limited tendency to segregate. Short-range ordering of Sb in terms of nearest neighbours pair formation was studied and we observed that Sb does not have an enhanced tendency to form pairs.

# Invited: Unveiling the effect of Growth Interruption Stages and Segregation Kinetics in ultrathin-GaAsSb films via AlAs markers

<sup>1</sup>\*D. F. Reyes<sup>1</sup>, V. Braza<sup>1</sup>, T. Ben<sup>1</sup>, S. Flores<sup>2</sup>, A. Gallego Carro<sup>2</sup>, L. Stanojević, M. Schwartz<sup>2</sup>, J. M. Ulloa<sup>2</sup>, D. González<sup>1</sup>.

\*lead presenter.

<sup>1</sup>daniel.fernandez@uca.es, University Research Institute on Electron Microscopy & Materials, (IMEYMAT), Universidad de Cádiz, 11510 Puerto Real (Cádiz), Spain.

<sup>2</sup> Institute for Optoelectronic Systems and Microtechnology (ISOM), Universidad Politécnica de Madrid, Ciudad Universitaria s/n, 28040. Madrid, Spain.

III-V-Sb materials are emerging as top contenders for enhancing device efficiency in the infrared spectrum due to their distinctive properties, such as tunability across a broad wavelength range (from 0.1 eV to 1.8 eV) and the capability to switch between type I and type II bandgap alignments. However, growing very thin films, such as quantum wells or superlattices, presents considerable challenges, primarily due to pronounced Sb segregation, which broadens both interfaces [1, 2]. Various growth strategies have been proposed in the literature to mitigate this issue for GaAsSb layers, such as exposing the surface to Sb fluxes before (soaking) or As fluxes after (desorption) the deposition of the active layer. In this study, we have quantitatively evaluated the impact of applying both growth interruption (GI) strategies, both combined and separately, on Sb segregation in thin GaAs<sub>0.95</sub>Sb<sub>0.05</sub> films with thicknesses ranging from 1 to 20 ML. To achieve this, we introduced AlAs markers to rigorously apply the 3-layers kinetic fluid model (3LKFM) for estimating segregation parameters using HAADF and EDX techniques in STEM mode [3].

The results indicate that in the absence of GI (sample R), Sb profiles exhibit Gaussian-like peaks whose maximum and peak position shift with increasing film thickness (see Fig 1a). Specifically, the AlAs markers reveal a consistent delay of 5 ML in the onset of the GaAsSb layer. Employing the soaking step results in more effective incorporation (sample S), enhancing the upward composition gradient, and advancing the film onset. However, applying only desorption stages (sample D) significantly impact the Sb profiles, with only thicker GaAsSb layers remaining. Combining both strategies (sample SD) produces squared profiles with higher Sb contents and sharper gradients, but the mechanism is more complex than a simple addition and subtraction of Sb amounts. 3LKFM simulations show that the segregation energy changes during layer growth, initially being higher but stabilizing around the same value for all cases. Sb-soaked samples achieve the segregation steady state much earlier than non-soaked samples.

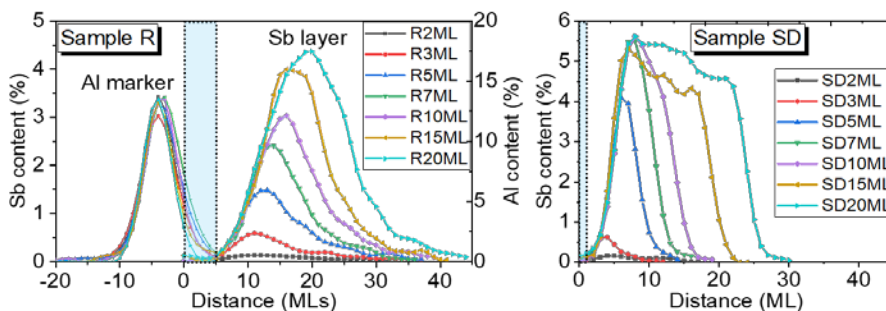


Figure 1: Overlapping compositional profiles of Sb along the direction of growth with different layer thicknesses for the R sample (left) and the SD sample (right).

1. D. Gonzalez et al., *Nanomaterials*, 13, (2023) 798. Doi: 10.3390/nano13050798
2. V. Braza et al. *Appl. Surf. Sci.*, 604, (2022) 154596. Doi: 10.1016/j.apsusc.2022.154596
3. S. Flores et al., *Appl. Surf. Sci.*, 607, (2023) 154966. Doi: 10.1016/j.apsusc.2023.158676

# SESSION 7



# Keynote: GaSb based Interband Cascade devices for spectroscopic applications

\*Weih, R., Nauschütz, J., Schäfer, N., Scheuermann, J. & Koeth, J.

\*lead presenter

robert.weih@nanoplus.com, nanoplus Advanced Photonics Gerbrunn GmbH, Oberer Kirschberg 4, Gerbrunn, Germany

Interband Cascade Lasers (ICLs) based on GaSb or InAs have evolved tremendously since their first scientific mention in 1995 [1]. Meanwhile the entire mid infrared spectral region from 2.7 to more than 6 $\mu\text{m}$  can be covered by devices that operate in continuous wave mode above room temperature. These pave the way for numerous spectroscopic applications in the industrial, environmental or medical field. In order to fulfill the demand for higher output power and tuneability various optimizations have been implemented within the last years. In the design of ICLs the most tremendous have been the introduction of the carrier rebalancing concept [2] and the mitigating of valence intersubband absorption [3] within the active quantum wells. Also, in the chip design of DFB lasers that are commonly used for spectroscopy various optimizations have been introduced that led to a significant improvement in device performance.

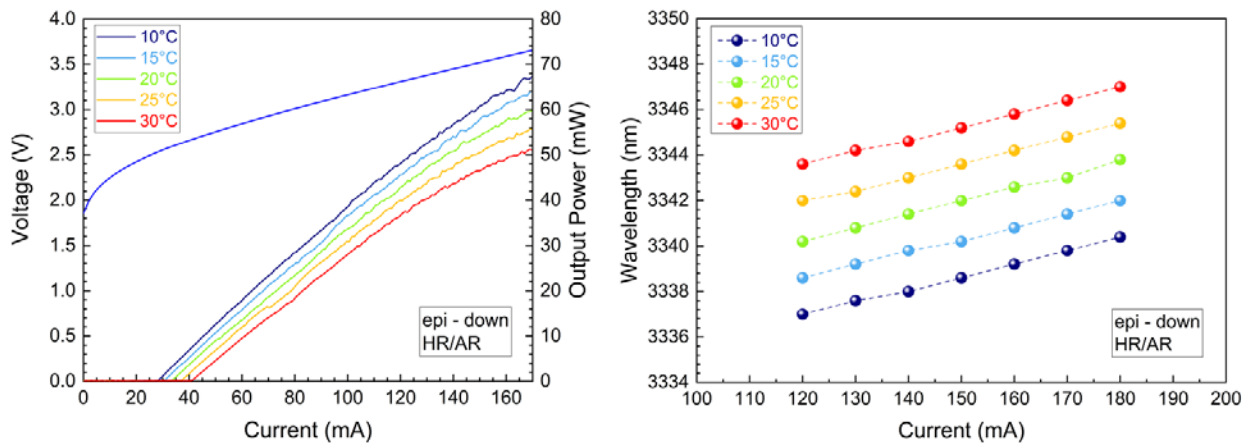


Figure 1: LIV curves and tuning behavior of a DFB ICL emitting around 3.34  $\mu\text{m}$ .

In the left side of the Figure 1 LIV curves for an epi down mounted DFB ICL are shown. At room temperature it emits more than 60mW of output power which is sufficient for most spectroscopic applications. In the right graph the wavelength tuning with current and operation temperature is shown. The DFB emits around 3.34 $\mu\text{m}$  and can cover a wavelength range of 10nm.

Band structure engineering within the 6.1 $\text{\AA}$  III-V semiconductor family also enables the realization of ICLEDs and ICDs that are valuable devices for spectroscopic applications. The talk will cover the latest developments and achievements in the field of commercially available ICLs, ICLEDs and ICDs.

[1] R.Q. Yang, "Infrared Laser Based on Intersubband Transitions in Quantum Wells," *Superlattices and Microstructures* **17**, No. 1 (1995).

[2] I. Vurgaftman, W.W. Bewley, C.L. Canedy, C.S. Kim, M. Kim, C.D. Merritt, J. Abell, J.R. Lindle and J.R. Meyer, "Rebalancing of internally generated carriers for mid-infrared interband cascade lasers with very low power consumption," *Nature Comm.* 2:585 (2011).

[3] H. Knötig, J. Nauschütz, N. Opacak, S. Höfling, J. Koeth, R. Weih, and B. Schwarz, "Mitigating Valence Intersubband Absorption in Interband Cascade Lasers," *Laser Photonics Rev.* 2200156 (2022).

# Keynote: Sb-based Type II superlattices for infrared detectors at IRnova

\*<sup>1,2</sup> D. Ramos, <sup>2</sup>L. Höglund, <sup>2</sup>M. Delmas, <sup>2</sup>R. Ivanov, <sup>2</sup>T. Kohl, <sup>2</sup>L. Bendrot, <sup>2</sup>L. Žurauskaitė, <sup>2</sup>D. Evans, <sup>2</sup>D. Rihtnesberg, <sup>2</sup>S. Högnadóttir, <sup>2</sup>S. Smuk, <sup>2</sup>A. Smuk, <sup>2</sup>S. Becanovic, <sup>2</sup>S. Almqvist, <sup>2</sup>P. Tinghag and <sup>2</sup>E. Costard

\*lead presenter

<sup>1</sup>david.ramos@ir-nova.se

<sup>2</sup> IRnova AB, Electrum 236 - C5, SE-164 40 Kista, Sweden

In the last decade, Sb-based Type II superlattice (T2SL) structures have evolved from an emerging technology to modern state-of-the-art infrared (IR) detectors. T2SL has proven to be an excellent industrial solution for manufacturing IR imaging sensors that cover the entire IR range: extended shortwave (eSWIR) 1-2.5  $\mu\text{m}$ , midwave (MWIR) 3-5.5  $\mu\text{m}$ , and very long wave (VLWIR) 8-14  $\mu\text{m}$ . These detectors surpass traditional IR detector materials in performance and scalability, enabling the development of sensors with higher operating temperatures and larger formats. This innovation reduces the need for bulky cryogenic cooling, resulting in low Size, Weight, and Power (SWaP) imaging systems that are both cost-effective and highly efficient.

This paper describes the T2SL technology and presents the detector development at IRnova for MWIR and eSWIR. First, the MWIR section presents the implementation of the T2SL technology in the formats of 640 x 512 - 15  $\mu\text{m}$  pitch, 1280 x 1024 - 10  $\mu\text{m}$  pitch and 7.5 and 5  $\mu\text{m}$  pitch arrays. Secondly, the eSWIR section validates the T2SL technology in a 640 x 512 - 15  $\mu\text{m}$  format and presents a route towards continued development HD detectors (2k x 0.5k - 15  $\mu\text{m}$  pitch). The MWIR advancements represent the first European-manufactured SWaP T2SL detector assembly and demonstrate its HD readiness, while the eSWIR developments target space applications within the EU-funded STEP project (Silicon and T2SL European collaboration for a non-dependent supply chain for large eSWIR focal plane arrays).

# SESSION 8



# Invited: Optical properties of InAs/GaSb and InAs/InAsSb superlattices for mid infrared detection: structural defects and band offset issue

<sup>1</sup>Rygała, M., <sup>2</sup>Zanon, J., <sup>3</sup>Bader, A., <sup>1</sup>Smółka, T., <sup>3</sup>Hartmann, F., <sup>3,4</sup>Flatté, M., and <sup>1\*</sup>Motyka, M.

<sup>1</sup>Department of Experimental Physics, Faculty of Fundamental Problems of Technology, Wrocław University of Science and Technology, 50-370 Wrocław, Poland

<sup>2</sup>Department of Applied Physics, Eindhoven University of Technology, 5612 AZ Eindhoven, Netherlands

<sup>3</sup>Julius-Maximilians-Universität Würzburg, Physikalisches Institut, Lehrstuhl für Technische Physik, Am Hubland, 97074 Würzburg, Germany

<sup>4</sup>Department of Physics and Astronomy, University of Iowa, Iowa City, Iowa 52242, USA

\*lead presenter

email: [marcin.motyka@pwr.edu.pl](mailto:marcin.motyka@pwr.edu.pl),

Modern optical gas detection systems utilize the technique of tunable laser absorption spectroscopy for different applications in science, manufacture, or medicine. Superlattice structures composed of semiconductors from the 6.1 Å family enable type-II band alignments and have the potential to exceed state of the art figure of merits of widely used infrared detectors. In this study, InAs/GaSb and InAs/InAsSb type-II superlattices were grown using molecular beam epitaxy and characterized using Fourier-transform infrared spectroscopy and pump-probe transient absorption technique. Photoluminescence (PL) spectra were obtained for all samples in 10 to 300K temperature range and then complemented with photorefectance (PR) measurements for characteristic temperatures to increase the sensitivity of the measurement for less optically active transitions. Regarding the InAs/GaSb the interface engineering was performed through Sb soaking and insertion of the InSb monolayer after each period of the superlattice. In the case of InAs/InAsSb superlattices three samples with different periods were investigated. Power dependence of PL allowed to connect the measured signals with e1-hh1 and defect related transitions. By comparing the transitions energies and calculated confined levels, we have studied the valence band offset.

In addition, pump-probe measurements were performed to investigate the dynamics of carrier relaxation and recombination processes in proximity of transition energies observed in previous experiments. The characteristic two decay times in pump-probe spectra have been determined for InAs/GaSb in contrast to InAs/InAsSb, where additional third process has been revealed.

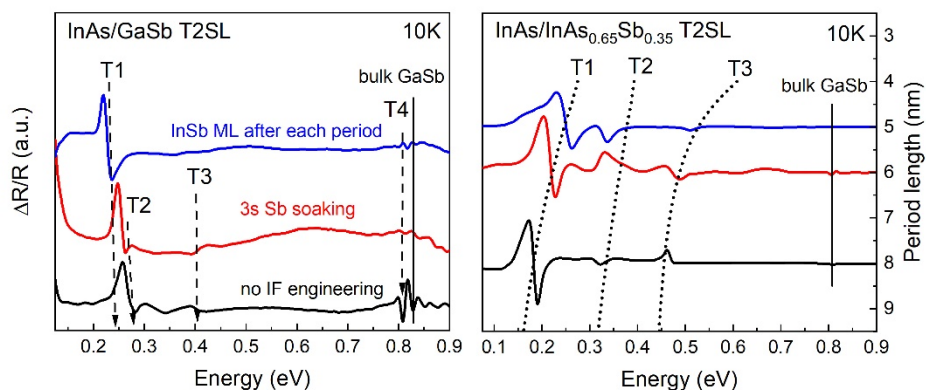


Figure 1. 10K Photorefectance spectra for InAs/GaSb (left) and InAs/InAsSb (right) superlattices

# Understanding Growth Kinetics of GaSb: Computational Modeling for Process Optimization

H. Husejini\*, M. Dauelsberg, M. Mukinovic, B. Schineller and M. Heuken  
h.husejini@aixtron.com  
AIXTRON SE, Dornkaulstr. 2, 52134 Herzogenrath, Germany

Having the smallest bandgaps among V-III materials makes antimonide-based compounds very attractive for mid-infrared light emitters, detectors, as well as long-wavelength optoelectronic devices such as thermophotovoltaics and lasers. The growth kinetics of these materials are poorly understood, and important thermodynamic and kinetic data are missing. The work presented is based on simulating gas-phase transport phenomena and surface kinetics using computational fluid dynamics (CFD). This approach involves computing fluid dynamics, heat transfer, and species mass transfer, including gas-phase chemistry and surface kinetics. A simplified 2D model is employed with a focus on adaptability to the AIXTRON Planetary Reactor<sup>®</sup>. The main objective of this research is to enhance our understanding of growth kinetics and reveal the main pathways leading to the growth of GaSb.

Metal-organic precursors like Trimethylgallium (TMGa), triethylgallium (TEGa), and trimethylantimony (TMSb) are used during the investigation of GaSb MOCVD growth. Relatively low V/III ratios of 1.29 and 1.5 are employed for the TMGa-TMSb and TEGa-TMSb chemistries, respectively. Parameter variations are carried out to distinguish between the effects of growth temperature, flow rate, precursor molar fraction, as well as V/III ratio. The temperature range is limited to 500-652°C, aligning with the constraints imposed by GaSb properties. A reduced reaction mechanism, considering homogeneous and heterogeneous reactions in the gas phase and at the growth surface, is incorporated into the model.

The modified TMGa-TMSb and TEGa-TMSb models align with simulation results from literature, confirming the model's robustness. Depending on the temperature and reactor geometry, the source species in the gas phase undergo complete or partial decomposition. For the TMGa-TMSb chemistry used in the Horizontal Tube Reactor, the simulated growth rate demonstrates a linear dependence on the TMGa mole fraction at 625°C due to slower decomposition of TMGa relative to TMSb, while it is independent of the TMSb mole fraction. On the other hand, the TEGa-TMSb growth rate exhibits a slight sublinear dependence on the group V precursor mole fraction and a slight linear dependence on the TEGa mole fraction at 625°C. Specific growth regimes associated with the TMGa-TMSb chemistry are identified, with the mass transport regime dominating at higher temperatures, above 596°C, while below this temperature, surface kinetics govern the growth process.

In the context of the AIX G4 Planetary Reactor<sup>®</sup>, the transition temperature is slightly shifted towards 620°C for the operating growth conditions. In the TEGa-TMSb chemistry, a slight increase in growth rate with temperature is reported. The growth rate demonstrates either (sub)linear dependence on the molar flow rate or remains independent of it in other cases, contingent upon the growth temperature. The main reaction pathway that leads to the GaSb growth for the TEGa-TMSb chemistry is identified. In the case of AIX G5, the growth process occurs only in the kinetically limited. The alignment of our simulation model with observed growth trends in a wide range of growth conditions serves as a foundation for process improvement and offers benchmarks for GaSb growth in industrial MOCVD reactors.

# Interband cascade lasers with hybrid plasmon-enhanced claddings

<sup>1</sup>Borislav Petrović \*, <sup>2</sup>Andreas Bader, <sup>2</sup>Josephine Naüschutz, <sup>3</sup>Takuma Sato, <sup>3</sup>Stefan Birner, <sup>2</sup>Robert Weih, <sup>1</sup>Fabian Hartmann, & <sup>1</sup>Sven Höfling  
\*lead presenter

borislav.petrovic@uni-wuerzburg.de

<sup>1</sup>Julius-Maximilians-Universität Würzburg, Physikalisches Institut, Lehrstuhl für Technische Physik, Am Hubland, 97074 Würzburg, Germany

<sup>2</sup>nanoplus Advanced Photonics Gerbrunn GmbH, Oberer Kirschberg 4, 97218 Gerbrunn, Germany

<sup>3</sup>nextnano GmbH, Konrad-Zuse-Platz 8, 81829 München, Germany

We present interband cascade lasers (ICLs) emitting at 5.2  $\mu\text{m}$  and 4.6  $\mu\text{m}$  with hybrid claddings and 5.0  $\mu\text{m}$  with  $\text{Al}_{0.85}\text{Ga}_{0.15}\text{As}_{0.07}\text{Sb}_{0.93}$  quaternary claddings. The 8-stage GaSb-based ICL emitting at 5.2  $\mu\text{m}$  with hybrid claddings composed of outer plasmon-enhanced  $\text{InAs}_{0.915}\text{Sb}_{0.085}$  and inner InAs/AlSb superlattice claddings, shows an increase in mode confinement of 11.2 % according to the simulation. This is a consequence of a significantly lower refractive index of plasmon-enhanced claddings. The threshold current density is 242  $\text{A}/\text{cm}^2$  in pulsed operation at room temperature. This is the lowest value reported to date for ICLs emitting at wavelengths longer than 5  $\mu\text{m}$ . We also report close to record value threshold power density of 840  $\text{W}/\text{cm}^2$ . The measured thermal resistance as low as 62  $\text{K}/\text{W}$  highlights improved heat dissipation of the hybrid superlattice plasmon-enhanced claddings. In addition, we compare InAs-based and GaSb-based ICLs with the same 12 stage active region emitting at 4.6  $\mu\text{m}$  employing the hybrid claddings of the same geometry and inner claddings consisting of InAs/AlSb superlattices, but different outer claddings: The InAs-based ICL employs plasmon enhanced n-type doped InAs layers while the GaSb-based ICL employs plasmon-enhanced n-type doped InAsSb claddings lattice matched to GaSb. Due to the lower refractive index of  $n^+$ -InAsSb ( $n=2.88$ ) compared to  $n^+$ -InAs ( $n=3.10$ ), and higher refractive index of separate confinement layers, the GaSb-based ICL shows a 3.8 % higher optical mode confinement in the active region compared to the InAs-based ICL. Experimentally, the GaSb-based ICL shows a 17.3 % lower threshold current density in pulsed operation at room temperature. Also presented is the influence of geometry and doping variation on confinement factors and calculated free carrier absorption losses in the GaSb-based ICL.

# SESSION 9



# Invited

## Magic alloys of Antimonide

<sup>1</sup>Kesaria, Manoj<sup>1\*</sup>

\*lead presenter

<sup>1</sup>e-mail address: [kesariam@cardiff.ac.uk](mailto:kesariam@cardiff.ac.uk), School of Physics and Astronomy, Cardiff University, Cardiff.

Next-generation optoelectronic infrared quantum sensing systems lack a high-performing single photon detector. Detecting single photons can enable long-range free-space communication where atmospheric transmission demands detection in a wavelength range where detector technology is unavailable. Worldwide, ongoing research is being conducted to develop new materials to fabricate infrared avalanche photodiodes. The challenge is to make reproducible thicker layers to make avalanche photodetectors (APD) operating in Giger mode. Thicker ternary, quarterly, and quinary random alloy (RA) or conventional bulk alloys of III-V are hampered by As and Sb intermixing and phase segregations. Digital or magic alloys are an alternative to overcome the bottleneck in developing thicker alloys. Magic alloys are digital alloys (DA),  $A_n B_m$ , where A and B are binary semiconductors. Digital alloying is a modulated beam growth technique that enables device reproducibility and manufacturability, which was impossible with conventional bulk alloys. Digital alloys are less sensitive to drift in growth parameters; they permit abrupt and reproducible changes in composition, emulating conventional alloys by building an SPSL exhibiting basic optoelectronic properties such as bandgap, refractive index, etc.

In my talk, I will present an overview of my contributions to group III antimonides, quantum wells, multiple quantum wells, complex quantum wells (CQW)/superlattice (SL), and short-period strained superlattice (SPSL) /digital or magic alloys.

# Multiband $k\cdot p$ Modeling of Quantum Transport in Interband Cascade Lasers and Detectors

<sup>1,2\*</sup>Takuma Sato, <sup>1</sup>Stefan Birner, <sup>2</sup>Christian Jirauschek, & <sup>3</sup>Thomas Grange

\* takuma.sato@nextnano.com

<sup>1</sup>nextnano GmbH, Germany, <sup>2</sup>Technical University of Munich, Germany

<sup>3</sup>nextnano Lab, France

Interband cascade lasers (ICLs) and detectors have shown promising properties for mid-infrared gas sensing applications. The threshold power density of ICLs is significantly lower than for its intersubband counterpart, the quantum cascade laser. ICLs therefore have the edge in portability and battery operation [1].

While electrostatic modeling has provided several design guidelines for the recombination region of ICLs (see poster presentation), inadequate understanding of the carrier transport through electron and hole injectors has thus far limited design optimization of the whole active region [1]. This necessitates carrier transport simulation considering quantum mechanical tunneling through barriers and non-equilibrium charge distribution.

We find the envelope functions of the energy eigenstates in heterostructures by an eight-band  $k\cdot p$  solver that includes strain effects. We developed a scheme to construct the non-equilibrium Green's function (NEGF) basis from selected eigenstates and implemented it to nextnano.NEGF [2] (Figure). Poisson's equation is solved self-consistently with the NEGF equations. The model thus reflects simultaneously the quantum transport, interband coupling, in-plane nonparabolicity, phase-scattering mechanisms and doping effects in interband tunneling devices.

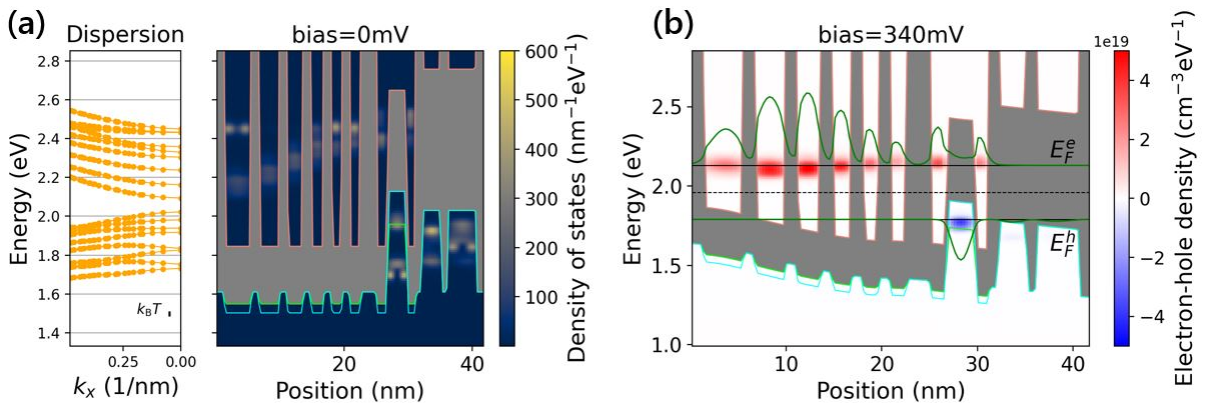


**Figure:** (a) In-plane dispersion (left) and local density of states (right) of electrons in the energy range relevant for transport (colormap) in one period of an ICL active region used in Ref. [5]. (b) Energy-resolved electron- and hole densities (colormap) simulated assuming constant quasi-Fermi levels (black solid lines) at a light-emitting bias. Green lines indicate electron- and hole densities integrated over energy.

## References

- [1] J. R. Meyer et al., *Photonics* **7**, 75 (2020).
- [2] T. Grange, *Phys. Rev. B* **89**, 165310 (2014).

# Sb-soaked InGaAs/GaAs quantum dots for enhanced hole g-tensor modulation

G. Barbieri\*, J.M. Llorens, A.G. Taboada, J.M. Ripalda, Y. González, B. Alèn  
\* g.barbieri@csic.es

*Instituto de Microelectrónica de Madrid, CNM (CSIC), C/Isaac Newton 8, PTM 28760 Tres Cantos, Madrid, Spain*

Epitaxially grown quantum dots (QDs) have emerged as a promising platform for solid-state quantum light sources, generating single photons and entangled photon pairs on demand, essential for secure quantum communication protocols and quantum information processing [1]. Moreover, a suitable choice of the material system and growth conditions also allow for tailorable optoelectronic properties and on-chip integration. However, to fully leverage their potential, precise coherent control over the quantum states in QDs is necessary. Such control is critical for implementing quantum entanglement, superposition, and error correction, thereby enabling reliable and scalable quantum networks. This can be achieved, for example, exploiting the coupling between the hole spin of a single QD to an external electric field through the spin-orbit interaction (SOC) [2]. Here, we investigate the optoelectronic and magneto optoelectronic properties of Sb-soaked InGaAs/GaAs QDs, which are proposed as ideal platforms for g-factor modulation since Sb presents the largest g-factor and SOC of group V elements.

Past studies [3,4] have shown that exposing InGaAs QDs to Sb before capping with GaAs (Sb-soaking) leads to larger and more homogeneous QDs thanks to increased ripening and surfactant properties of Sb, with Sb being incorporated mostly at the tip. We first confirm this by measuring photoluminescence (PL) and time-resolved PL, which show a redshift towards the telecom O-band and an increase in the radiative lifetime. We fit the inhomogeneously broadened spectra with our own 8-band k-p-based structural parameter extraction tool, and use the output to predict ensemble polarization-resolved magneto PL with nextnano [5], in excellent agreement with the experiment. Finally, we argue that thanks to both the large size and Sb segregated at the tip, these Sb-soaked InGaAs/GaAs QDs are an ideal platform for hole g-factor modulation and propose a device layout based on [6].

[1] C. Y. Lu and J. W. Pan, Quantum-Dot Single-Photon Sources for the Quantum Internet, *Nat. Nanotechnol.* 16, 1294 (2021).

[2] A. R. da Cruz and M. E. Flatté, Dissipationless Circulating Currents and Fringe Magnetic Fields Near a Single Spin Embedded in a Two-Dimensional Electron Gas, *Phys. Rev. Lett.* 131, 086301 (2023).

[3] Taboada, Alfonso G., et al. "Structural and optical changes induced by incorporation of antimony into InAs/GaAs (001) quantum dots." *Physical Review B* 82.23 (2010): 235316.

[4] Taboada, A. G., et al. "Effect of Sb incorporation on the electronic structure of InAs quantum dots." *Physical Review B* 88.8 (2013): 085308.

[5] Birner, Stefan, et al. "Nextnano: general purpose 3-D simulations." *IEEE Transactions on Electron Devices* 54.9 (2007): 2137-2142.

[6] Xiang, Zi-Heng, et al. "A tuneable telecom wavelength entangled light emitting diode deployed in an installed fibre network." *Communications Physics* 3.1 (2020): 121.

# Invited: Quantum Spin Hall Effect in Antimonide-based type-II Heterostructures

F. Hartmann<sup>1\*</sup>, M. Meyer<sup>1</sup>, T. Fährdrich<sup>1</sup>, S. Schmid<sup>1</sup>, A. Wolf<sup>1</sup>, S. S. Krishtopenko<sup>1,2</sup>, B. Jouault<sup>2</sup>, G. Bastard<sup>1,3</sup>, F. Tepe<sup>2</sup>, and S. Höfling<sup>1</sup>

<sup>1</sup>*Julius-Maximilians-Universität Würzburg, Physikalisches Institut and Würzburg-Dresden Cluster of Excellence ct.qmat, Lehrstuhl für Technische Physik, Am Hubland, 97074 Würzburg, Germany*

<sup>2</sup>*Laboratoire Charley Coulomb (L2C), UMR 5221 CNRS-Université de Montpellier, F-34095, Montpellier, France*

<sup>3</sup>*Physics Department École Normale Supérieure, PSL 24 rue Lhomond, 75005 Paris, France*

\*fabian.hartmann@uni-wuerzburg.de

Topological Insulators (TIs) exhibiting the Quantum Spin Hall effect (QSHE) have emerged as promising candidates for next-generation electronic devices due to their unique electronic properties of an insulating bulk and helical edge channels [1-3]. For a potential usage in device applications, the TI needs to display certain characteristics such as a scalability and reproducibility, a robustness of the helical edge channels against temperature and a tuning possibility (e.g., with electric field). Despite many material systems were predicted to host the QSHE and showed some of these characteristics, none of them could exhibit all of them [1,2]. One prominent example are 2D TIs based on InAs/GaSb bilayer quantum wells. They profit from their compatibility with the semiconductor industry and major growth and processing technology developed. Moreover, the possible phase transition between a TI and normal insulating (NI) phase [4] and the rather temperature-insensitive band ordering [5] make this material system interesting for potential device applications.

By adding another InAs-layer to the BQW, a symmetrical InAs/Ga(In)Sb/InAs trilayer quantum well (TQW) can be formed. Dependent on the individual quantum well thicknesses, a rich phase diagram emerges with either direct or indirect inverted band gaps, gapless phases (semi metallic) or massless Dirac fermions. TQWs are appealing because of the predicted band gap energies up to 60 meV for highly strained quantum wells [6] enabling high temperature operation with reduced bulk conductivity. We will discuss InAs/GaSb/InAs triple quantum wells with different InAs quantum well thicknesses ranging from 8.0 to 13.5 nm and how to experimentally ascertain the rich phase diagram in this material system [7]. Gate voltage and temperature dependent transport measurements reveal distinct transport signatures between samples designed from the trivial-insulating, the topological-insulating, up to the semi-metallic phase. Two-carrier transport together with pronounced Van Hove singularities are observable only for the samples grown in the topological-insulating phase and if camelback-like dispersions are present in the hybridized valence or conduction band. The different shaping and the amount of Van Hove singularities deliver also information about a turning point inside the topological-insulating phase.

## References:

- [1] M. König et al., *Science* **318**, 766 (2007).
- [2] S. Wu et al., *Science* **359**, 76 (2018).
- [3] L. Du et al., *Phys. Rev. Lett.* **114**, 096802 (2015).
- [4] F. Qu et al., *Phys. Rev. Lett.* **115**, 036803 (2015).
- [5] M. Meyer et al., *Phys. Rev. B* **104**, 085301 (2021).
- [6] S.S. Krishtopenko et al., *Sci. Adv.* **4** 7529 (2018)
- [7] S. Schmid et al. *Phys. Rev. B* **105**, 155304 (2022)

# POSTER SESSION



# P1: Random alloy effects in GaAsSb and related alloys

<sup>1</sup>\*Phan, A.-L., <sup>2</sup>Pecchia, A., <sup>1</sup>Di Vito, A. & <sup>1</sup>Auf der Maur, M.

\*lead presenter

<sup>1</sup> anh.luan.phan@uniroma2.it, University of Rome “Tor Vergata”, Italy

<sup>2</sup> ISMN-CNR, Italy

Many optoelectronic materials and devices involve disordered structures like random semiconductor alloys or alloy-like configurations at the hetero-interfaces, in which the chemical species and the strain profiles are complicated. Moreover, the realistic distribution of chemical elements in such alloyed structures can be in a non-uniform manner, adding more complexities to the task of predicting their electronic and optical properties. These properties require the calculations on large supercells containing  $10^4$ - $10^6$  atoms because, for example, the carrier localization might happen over several nanometers and the superlattices, quantum dots or similar structures are also of at least nanometer scale. Therefore, an efficient atomistic method to simulate these materials which account properly for the random alloy disorder's effects is desirable. In such a situation, the empirical tight-binding (ETB) method has been proven to be a good balance between the required accuracy and the computational cost.

We apply a recent ETB scheme proposed by Tan et al. [1], which advances a widely used ETB scheme by Jancu et al. [2] in dealing with the complexities present in alloyed structures, to the typical GaAsSb alloy and other related ones like InAsSb and InGaSb in order to investigate the impacts of random alloys on electronic and optical aspects of these materials. Our ETB results for the band gap variations of these alloys align excellently with the experimentally measured data and reconfirm the large bandgap bowing and the presence of the gap minima in the cases of GaAsSb and InAsSb. Furthermore, we investigate how the possible non-uniformity of alloy distribution which favors the formation of clusters can affect the electronic and optical quality of the realistic samples. Taking GaAsSb as a specific study case, the ETB simulations show that the non-uniformity decreases even further the band gap values, making the bandgap bowing parameter at small Sb-concentration larger than that in the case of uniformly random GaAsSb alloy. The localization of hole states in GaAsSb is also remarkably enhanced by increasing non-uniformity, while that of electron states is nearly unchanged. This enhanced localization of the charge carriers in turn is intimately related to the significant degradation of the optical transition in the GaAsSb alloy samples when non-uniformity is present, especially for those with small Sb-concentration. In addition, the non-uniformity also broadens the emission spectra of the samples. Those simulation predictions are consistent with the experimental observations in [3]. We emphasize that the simulation procedure we carried out is not limited to GaAsSb but can also be applied to other alloys.

[1] Y. Tan, M. Povolotskyi, T. Kubis, T. B. Boykin, and G. Klimeck, “Transferable tight-binding model for strained group IV and III-V materials and heterostructures,” *Phys. Rev. B*, vol. 94, p. 045311 (2016).

[2] J.-M. Jancu, R. Scholz, F. Beltram, and F. Bassani, “Empirical sp<sup>3</sup>s\* tight-binding calculation for cubic semiconductors: General method and material parameters,” *Phys. Rev. B*, vol. 57, pp. 6493–6507 (1998).

[3] X. Gao, Z. Wei, F. Zhao, Y. Yang, R. Chen, X. Fang, J. Tang, et al. “Investigation of Localized States in GaAsSb Epilayers Grown by Molecular Beam Epitaxy.” *Scientific Reports* 6, no. 1, p. 29112 (2016).

## **P2: Influence of interface intermixing on carrier dynamics in type-II InAsSb/GaAsSb W-quantum wells emitting in mid-infrared**

<sup>1</sup>\*Smołka, T., <sup>1</sup>Rygała, M., <sup>1</sup>Ryczko, K., <sup>2</sup>Bader, A., <sup>2</sup>Hartmann, F., <sup>2</sup>Petrovic, B., <sup>2</sup>Höfling, S. & <sup>1</sup>Motyka, M.

<sup>1</sup>Department of Experimental Physics, Faculty of Fundamental Problems of Technology, University of Science and Technology, 50-370 Wrocław, Poland

<sup>2</sup>Julius-Maximilians-Universität Würzburg, Physikalisches Institut, Lehrstuhl für Technische Physik, Am Hubland, 97074 Würzburg, Germany

\*lead presenter

email: [tristan.smolka@pwr.edu.pl](mailto:tristan.smolka@pwr.edu.pl)

Interband cascade lasers (ICLs) are a type of semiconductor laser that operates in the mid-infrared region of the electromagnetic spectrum. These lasers possess unique characteristics that make them crucial for a variety of applications, including gas sensing, spectroscopy, medical diagnostics, and communication. ICLs feature a cascade structure composed of multiple quantum wells, which enables them to achieve high efficiency, low threshold currents, and continuous-wave operation at room temperature. However, there is room for further optimization of the active region. In this study, we will examine the influence of tensile and compressive strain on the electronic structure and carrier dynamics.

The research involves transient absorption (TA) pump-probe measurements of type-II WQW InAsSb/GaAsSb/InAsSb structures designed for mid-infrared interband cascade lasers emitting near 3.5  $\mu\text{m}$ . The objective is to investigate the fundamental carrier dynamics in these material systems, which is critical for their potential applications in mode-locked lasers. TA measurements were conducted to assess the effect of applying compressive or tensile strain in quantum wells on carrier lifetimes, particularly concerning fundamental transitions and other interface-related ones. Additionally, the TA measurements show significant correlations between soaking time in the growth process and carrier lifetime.

Furthermore, photoreflectance (PR) and photoluminescence (PL) measurements were employed to study the band structure and optical properties of the samples. Both the PR and PL spectra displayed pronounced signals near 3.3  $\mu\text{m}$ , corresponding to the fundamental type-II transition of the quantum wells, along with additional signals (observed in PL) related to potential interface-atom intermixing processes. The observed optical transitions and their energies aligned well with theoretical calculations using the 8kp formalism.

# P3: Triple V-shaped quantum wells for 7.5 $\mu\text{m}$ emitting Interband cascade lasers

<sup>1</sup>Borislav Petrović \*, <sup>3</sup>Takuma Sato, <sup>3</sup>Stefan Birner, <sup>2</sup>Robert Weih, <sup>1</sup>Fabian Hartmann, & <sup>1</sup>Sven Höfling

\*lead presenter

borislav.petrovic@uni-wuerzburg.de

<sup>1</sup>Julius-Maximilians-Universität Würzburg, Physikalisches Institut, Lehrstuhl für Technische Physik, Am Hubland, 97074 Würzburg, Germany

<sup>2</sup>nanoplus Advanced Photonics Gerbrunn GmbH, Oberer Kirschberg 4, 97218 Gerbrunn, Germany

<sup>3</sup>nextnano GmbH, Konrad-Zuse-Platz 8, 81829 München, Germany

We present a design of triple V-shaped, type II-quantum wells (QWs) composed of AlSb/InAs/Ga<sub>0.6</sub>In<sub>0.4</sub>Sb/InAsSb/Ga<sub>0.6</sub>In<sub>0.4</sub>Sb /InAs/AlSb layers featuring an enhanced overlap integral of electron and hole wave functions. The transition energy and overlap integral were calculated for different combination of thicknesses of InAs, Ga<sub>0.6</sub>In<sub>0.4</sub>Sb and InAsSb layers as well as different arsenic compositions in InAsSb layer. In contrast, we calculated overlap integrals and transition energies in a commonly employed W-shaped AlSb/InAs/Ga<sub>0.6</sub>In<sub>0.4</sub>Sb /InAs/AlSb QW for different thicknesses of InAs and Ga<sub>0.6</sub>In<sub>0.4</sub>Sb layers. At the wavelength of approximately 7.5  $\mu\text{m}$ , the overlap integral of triple V-shaped QW has shown an increase of the overlap integral by 33.2 %. This enhancement could potentially extend the window of room temperature pulsed operation of interband cascade lasers from current limit of 6.8  $\mu\text{m}$ .

# P4: Insight into GaSb Growth: Implications for Industrial MOCVD Reactors

H. Husejني\*, M. Dauelsberg, M. Mukinovic, B. Schineller and M. Heuken

h.husejني@aixtron.com

AIXTRON SE, Dornkaulstr. 2, 52134 Herzogenrath, Germany

Antimonide-based compounds are highly desirable for mid-infrared light emitters, detectors, and long wavelength optoelectronic devices such as thermophotovoltaics and lasers. However, understanding the growth kinetics of these materials remains a challenge due to the lack of experimental as well as important thermodynamic and kinetic data. This study employs computational fluid dynamics (CFD) to simulate gas-phase transport phenomena and surface kinetics. A simplified 2D model, tailored for the AIXTRON Planetary Reactor®, is utilized to investigate GaSb growth using metal-organic precursors like Trimethylgallium (TMGa), triethylgallium (TEGa), and trimethylantimony (TMSb). The research focuses on elucidating growth kinetics and identifying key pathways for GaSb growth. Parameter variations, including growth temperature, flow rate, precursor molar fraction, and V/III ratio, are explored within a temperature range of 500-652°C. A reduced reaction mechanism, encompassing homogeneous and heterogeneous reactions, is incorporated into the model.

Simulation results for Horizontal Tube Reactor are compared with literature data, confirming the model's reliability. The study reveals temperature-dependent growth regime at lower temperature, with mass transport dominating at higher temperatures (>596°C) for the TMGa-TMSb chemistry. The main reaction pathway for GaSb growth in the TEGa-TMSb chemistry is identified. In the case of the AIX G4 Planetary Reactor®, the data show a slight shift of the transition temperature towards 620°C. Conversely for AIX G5, the growth process occurs only in the kinetically limited regime. These findings provide insights for process improvement and serve as benchmarks for GaSb growth in industrial MOCVD reactors.

# P5: Electronic structure of GaSb/AlGaSb quantum dots formed by filling droplet-etched nanoholes

<sup>1\*</sup>L. Leguay, <sup>2</sup>A. Chellu, <sup>2</sup>J. Hilska, <sup>1</sup>A. Schliwa, <sup>2</sup>M. Guina, <sup>2</sup>T. Hakkarainen  
<sup>1\*</sup>[l.leguay@tu-berlin.de](mailto:l.leguay@tu-berlin.de), Institute of Solid-State Physics, TU Berlin, Germany  
<sup>2</sup>Optoelectronics Research Center, Physics unit, Tampere, Finland

Semiconductor quantum dots (QDs) show tremendous potential for the generation of single and entangled photons required for quantum communication protocols such as free-space and fiber-based quantum key distribution (QKD) in the telecom C-band. Integrating telecom-wavelength QDs with Si photonics enables scalable quantum photonic integrated circuits, minimizing waveguide propagation losses. Strain-free GaAs/AlGaAs QDs fabricated via local droplet etching (LDE) demonstrate state-of-the-art performance in single photon indistinguishability and entanglement fidelity in the 680 – 800 nm range<sup>1</sup>.

This study focuses on simulations of highly uniform GaSb/AlGaSb QDs grown via LDE<sup>2,3</sup>, emitting in the telecom S-band with a narrow ensemble emission linewidth. We employ the nextnano++ software<sup>4</sup> to investigate the energy structure, radiative transition energies, carrier movement barriers, and optical transitions of the QDs using both the effective mass method and 8-band k.p model, uncovering insights into band structures, dipole transitions, and system dimensions, which are crucial to understand GaSb/AlGaSb QD integration in quantum photonic applications.

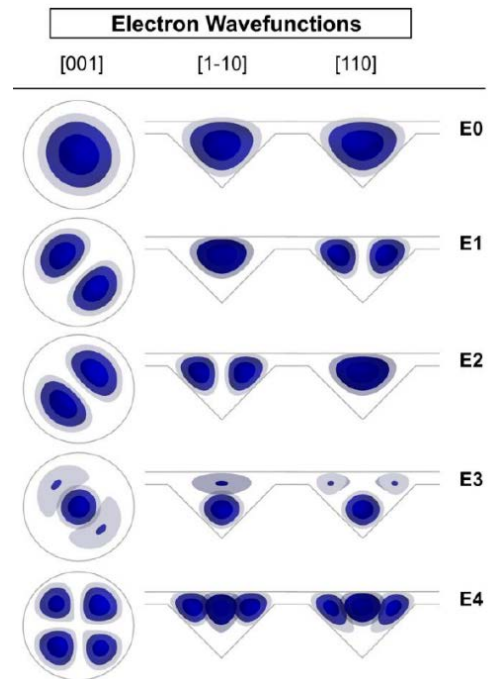


Figure 2:  $\Gamma$ -electron wavefunctions (probability densities) of the quantum dot. The viewing axes are [110], [1-10], and [001].

<sup>1</sup>M. Gurioli, Z. Wang, A. Rastelli, T. Kuroda, S. Sanguinetti, Nature Materials 18, 799 (2019).

<sup>2</sup>J. Hilska, A. Chellu, T. Hakkarainen, Cryst. Growth Des. 21 1917–1923 (2021).

<sup>3</sup>A. Chellu, J. Hilska, J.-P. Penttinen, T. Hakkarainen, APL Materials 9, pp. 051116 (2021).

<sup>4</sup>S. Birner et al, IEEE Trans. Electron Dev. 54, 2137 (2007).

# P6: X-Ray nanoprobe investigation of GaAsSb-capped InAs QDs

<sup>1,\*</sup>Malte Schwarz, <sup>2</sup>Fernanda Malato, <sup>2</sup>Jaime Dolado, <sup>1</sup>Alejandro Gallego Carro, <sup>2</sup>Gema Martinez-Criado and <sup>1</sup>Jose M. Ulloa

\* lead presenter, [malte.schwarz@upm.es](mailto:malte.schwarz@upm.es)

<sup>1</sup>Institute for Optoelectronic Systems and Microtechnology (ISOM), Universidad Politécnica de Madrid, Avda. Complutense 30, 28040 Madrid, Spain

<sup>2</sup>Experiments Division, X-ray Nanoprobe Group, European Synchrotron Radiation Facility, 38043 Grenoble, France

The implementation of quantum dots (QDs) can boost solar cells beyond their current efficiency limits. Further, a thin GaAsSb capping layer on InAs/GaAs QDs allows to tune the QD strain, morphology, band alignment and radiative carrier lifetimes. An in-depth material analysis of these structures revealed an Sb accumulation on top of the QDs for high Sb contents but is currently limited to cross-sectional techniques and probing of few QDs.

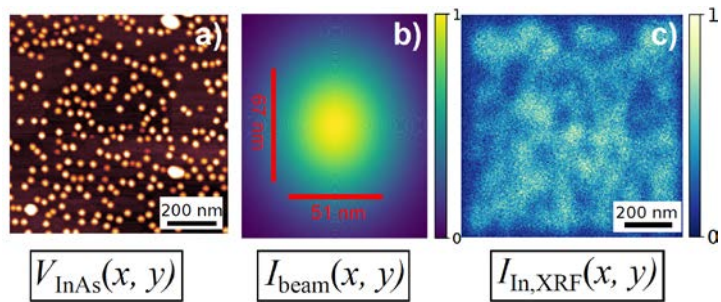


**Figure 1:** Predicting the XRF signal of a buried QD layer: a) atomic force microscopy (AFM) scan of surface QDs. b) Gaussian beam profile corresponding to experimentally determined FWHM of 51 nm and 67 nm c) Estimated In-XRF signal with the addition of shot-noise. Areas of high and low intensity correspond to areas of high and low QD density, respectively.

This work studies GaAsSb-capped InAs quantum dots with a multimodal hard X-ray nanoprobe. We compare two samples of 8% and 28% Sb content in the CL (hereinafter referred to as CL8 and CL28) leading to a type-I and type-II band alignment, respectively. As a reference, we also measured a sample of GaSb. We show how X-ray fluorescence (XRF) maps can be used to navigate in the QD plane (Fig. 1) and the local structure is investigated by X-ray absorption near edge structure (XANES). The acquired In-XRF maps (Fig. 2a) reflect the underlying buried QDs, and its correlation with Sb-XRF maps (Fig. 2b) is analyzed.

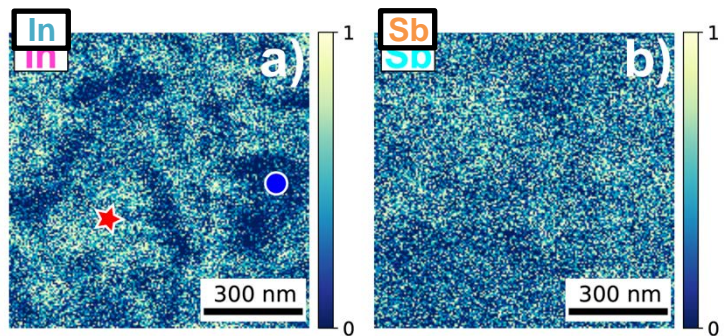


**Figure 2:** XRF maps of a) In  $K\alpha$  emission and b) Sb  $K\alpha$  emission from sample CL28. The red star in a) is placed in an area of high In signal, thus indicates emission by underlying QDs, while the blue circle is placed in an area of low In signal, indicating low QD density, thus emission from the WL.

Future work and spatially resolved spectroscopy would require QDs of lower density which are further of great interest regarding their use in quantum devices.

# P7: Optimization of Optical Transitions in Infrared Interband Devices with Multiband k·p Model

<sup>1,2\*</sup>Takuma Sato, <sup>1</sup>Stefan Birner, <sup>2</sup>Christian Jirauschek, & <sup>3</sup>Thomas Grange

\* takuma.sato@nextnano.com

<sup>1</sup>nextnano GmbH, Germany, <sup>2</sup>Technical University of Munich, Germany

<sup>3</sup>nextnano Lab, France

Interband cascade lasers (ICLs) and interband cascade infrared photodetectors (ICIPs) rely on electron-hole recombination and generation, respectively, in quantum wells with small effective band gaps, often consisting of antimonide compounds. Theoretical modeling based on the eight-band k·p Schrödinger-Poisson coupled equations provides design guidelines for the quantum wells [1-3].

We present concrete examples of the optimization of ICL active regions. We calculate optical gain spectrum by Fermi's golden rule. The optical transition involving valence subbands largely depends on light polarization and requires intricate treatment of the dependence on the in-plane momentum. An optimized doping profile and concentration improves the gain calculated under quasi-equilibrium assumption (Figure), in agreement with measurements [5].

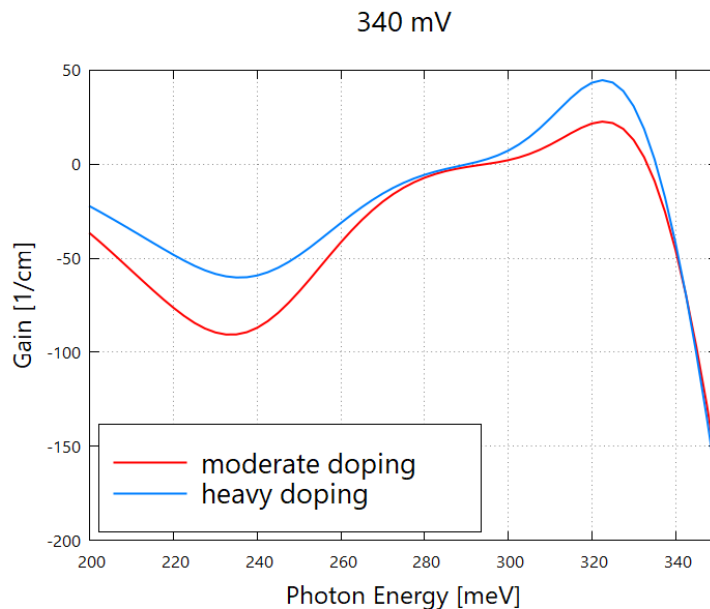


Figure: Semiclassical gain spectrum of an ICL under bias for different doping profiles.

## References

- [1] B. Petrović, et al., Appl. Phys. Lett. (accepted).
- [2] K. Ryczko et al., J. Appl. Phys. **114**, 223519 (2013).
- [3] H. Knötig et al., Laser Photonics Rev. 2022, **16**, 2200156 (2022).
- [4] A. Bader et al., Appl. Phys. Lett. **121**, 041104 (2022).
- [5] I. Vurgaftman et al., Nat. Comm. **2**, 1-7 (2011)

# P8: MagnetoOptoelectronic properties of local droplet etched GaSb/AlGaSb quantum dots emitting in the S-band

G. Barbieri\*<sup>1</sup>, J.M. Llorens<sup>1</sup>, L. Leguay<sup>2</sup>, A. Schliwa<sup>2</sup>, A. Chellu<sup>3</sup>, J. Hilska<sup>3</sup>, T. Hakkarainen<sup>3</sup>, S. Birner<sup>4</sup> and B. Alén<sup>1</sup>.

\* g.barbieri@csic.es

<sup>1</sup> Instituto de Microelectrónica de Madrid, CNM (CSIC), C/Isaac Newton 8, PTM 28760 Tres Cantos, Madrid, Spain

<sup>2</sup> Institut für Festkörperphysik, Fakultät II, Technische Universität Berlin, Hardenbergstraße 36, 10623, Berlin, Germany.

<sup>3</sup> Optoelectronics Research Center, Physics unit, Korkeakoulunkatu 3, 33720, Tampere, Finland.

<sup>4</sup> nextnano GmbH, Lichtenbergstr. 8, Garching b. München, 85748, Germany.

Non-classical light emission, tailorable optoelectronic properties and on-chip integration have made semiconductor quantum dots (QDs) a strong candidate and extensively studied platform for quantum communication and photonic quantum computation. Compared to QDs grown with the Stranski-Krastanov method (SK), QDs grown by local droplet etching (LDE) allow for a higher control over the structural properties and the composition profile [1]. These QDs are lattice matched, which results in vanishing fine structure splitting and narrow exciton linewidths, properties have enabled to demonstrate state-of-the-art performance in terms of photon indistinguishability and entanglement in the 680–800nm spectral range [2]. Recently, a novel GaSb/AlGaSb QD system has been introduced [3-5]. The related nanostructures emit at 1.5  $\mu\text{m}$ , close to the telecom C-band, where optical fibers offer lowest absorption and wave packet dispersion, and can be monolithically integrated on Silicon by interfacial misfit dislocation arrays. However, in order to coherently control the quantum state of the quantum dot, numerous quantum gate operation protocols rely on the application of external fields.

With this in mind, we set out to perform polarization-resolved magneto photoluminescence and compared the results with realistic 8-band k-p simulations with nextnano [6]. We found that the system's symmetry and lack of strain, together with the relatively large QD size, result in strong intermixing of the hole states, separated by just a few meV. This means that the eh-pair energy scales predominantly reflect those of the electrons, which can radiatively recombine with a near-continuum of hole states and which is also reflected in the magnetic dispersion. Interestingly, even a very low In content (3%) added to the QDs seems to assign a predominantly HH nature to the lowest states of the CB.

[1] Gurioli, Massimo, et al. "Droplet epitaxy of semiconductor nanostructures for quantum photonic devices." *Nature materials* 18.8 (2019): 799-810.

[2] Huber, Daniel, et al. "Strain-tunable GaAs quantum dot: A nearly dephasing-free source of entangled photon pairs on demand." *Physical review letters* 121.3 (2018): 033902.

[3] Chellu, Abhiroop, et al. "Highly uniform GaSb quantum dots with indirect-direct bandgap crossover at telecom range." *APL Materials* 9.5 (2021).

[4] Leguay, Lucie, et al. "Unveiling the electronic structure of GaSb/AlGaSb quantum dots emitting in the third telecom window." *Materials for Quantum Technology* 4.1 (2024): 015401.

[5] Michl, Johannes, et al. "Strain-Free GaSb Quantum Dots as Single-Photon Sources in the Telecom S-Band." *Advanced Quantum Technologies* 6.12 (2023): 2300180.

[6] Birner, Stefan, et al. "Nextnano: general purpose 3-D simulations." *IEEE Transactions on Electron Devices* 54.9 (2007): 2137-2142.

# P9: Computationally efficient $\mathbf{k}\cdot\mathbf{p}$ calculations for semiconductor superlattices: plane waves and multi-band Hamiltonians

\*Cónal Murphy<sup>1,2</sup>, Eoin P. O'Reilly<sup>1,2</sup> and Christopher A. Broderick<sup>2,1</sup>

<sup>1</sup>Tyndall National Institute, University College Cork, Dyke Parade, Cork T12 R5CP, Ireland

<sup>2</sup>School of Physics, University College Cork, Cork T12 YN60, Ireland

\* [conal.murphy@umail.ucc.ie](mailto:conal.murphy@umail.ucc.ie)

We develop a calculational framework to explicitly calculate optoelectronic properties of III-V superlattices (SLs) via a multi-band  $\mathbf{k}\cdot\mathbf{p}$  Hamiltonian in conjunction with the plane wave expansion method. [1] The periodicity of the plane wave basis states allows computation of the SL miniband structure using a calculational supercell consisting of a single SL period. This approach is generally applicable to semiconductor systems whose constituent material bulk band structures can be well described via a multi-band  $\mathbf{k}\cdot\mathbf{p}$  Hamiltonian. This provides a computational inexpensive platform to perform high-throughput calculations of optoelectronic properties to support the design of LEDs, lasers and photodetectors.

In this poster we will detail the application of this framework to two heterostructures operating in the application rich mid-infrared spectral range.

Firstly, we examine radiative recombination in InAs/GaSb SLs. In a technically challenging wavelength range [2], prototypical inter-band cascade LEDs based on InAs/GaSb SLs operating at room temperature [3] have demonstrated promise. Using calculated SL eigenstates we explicitly compute spontaneous emission and the radiative recombination rate. For an exemplar InAs/GaSb SL we provide detailed analysis of the impact of miniband on the radiative recombination rate. We then perform high-throughput calculations to maximise room temperature radiative recombination at fixed wavelength in the 3.5 – 7  $\mu\text{m}$  wavelength range.

Secondly, we investigate optical absorption in InAs/InAs<sub>1-x</sub>Sb<sub>x</sub> strain-balanced SLs. We extend the above model to compute optical absorption while explicitly incorporating the SL minibands. We consider pseudomorphic SLs grown on a GaSb buffer layer [4], and undertake a systematic optimisation of the near-band-edge optical absorption in strain-balanced SLs possessing tensile-strained InAs and compressively strained InAs<sub>1-x</sub>Sb<sub>x</sub> layers. We systematically vary the InAs and InAs<sub>1-x</sub>Sb<sub>x</sub> layer thicknesses and Sb composition  $x$ , to identify structures with a desired cutoff wavelength. We do this for wavelengths close to 5  $\mu\text{m}$  with an assumed operating temperature of 150 K. We carry out detailed analysis of the trends in optical absorption and quantify the potential benefit of structural optimisation.

[1] C. Murphy, E. P. O'Reilly and C. A. Broderick, *J. Phys. D: Appl. Phys.* **57**, 035103 (2023)

[2] T. D. Eales, I. P. Marko, B. A. Ikyo, A. R. Adams, S. Arafim et al., *IEEE J. Sel. Topics Quantum Electron.* **23**, 1-9 (2017)

[3] Y. Zhou, Q. Liu, X. Chai, Z. Xu, A. Krier, and L. He, *Appl. Phys. Lett.* **114**, 253507 (2019)

[4] E. Delli, P. D. Hodgson, M. Bentley, E. Repiso, A. P. Craig, Q. Lu, R. Beanland, A. R. J. Marshall et al., *Appl. Phys. Lett.* **117**, 131103 (2020)

# P10: Investigating crystal defects in quantum rings using electron microscopy

<sup>1</sup>\*Alvarado Cesar, F., <sup>2</sup>Acar, G., <sup>2</sup>Hodgson, P.D., Hayne, M. & <sup>1</sup>Beanland, R.  
\*lead presenter

<sup>1</sup>Francisco.Alvarado-Cesar@warwick.ac.uk, University of Warwick, United Kingdom

<sup>2</sup> University of Lancaster, United Kingdom

GaSb quantum rings (QRs) are nanoscale semiconductor structures with significant potential for use as single-photon sources or active regions in light-emitting diodes and lasers operating within the 1260–1675 nm telecommunication band[1]. Achieving these wavelengths has been challenging with other GaAs-based devices. However, growing GaSb QRs on GaAs substrates presents challenges due to the substantial lattice mismatch between GaAs (5.65 Å) and GaSb (6.1 Å), which can induce crystal faults. Minimizing defect density is crucial for the optimal performance of any device. Advanced electron microscopy techniques, such as electron contrast imaging (ECCI) and dark-field diffraction contrast transmission electron microscopy (TEM) imaging, are essential for understanding crystalline defects.

ECCI, a non-destructive scanning electron microscopy (SEM) technique, is effective for detecting defects in single-crystal semiconductors. By tilting the sample to satisfy Bragg conditions, electron beam penetration increases, a phenomenon known as channeling. Near defects, local rotation of the crystal planes alters the channeling, making defects visible[2]. In TEM, defects become visible in diffraction contrast images due to similar channeling effects. Additionally, cross-sectional dark-field imaging under diffraction conditions provides chemical sensitivity in III-V materials, which is valuable for characterizing epitaxial growth.

In this study, we employed ECCI and dark-field  $g = 002$  imaging to investigate the types and origins of defects in GaSb QRs. The sample was grown on a GaAs substrate with GaSb quantum rings embedded within GaAs/Al<sub>x</sub>Ga<sub>1-x</sub>Sb Bragg mirrors using molecular beam epitaxy (MBE).

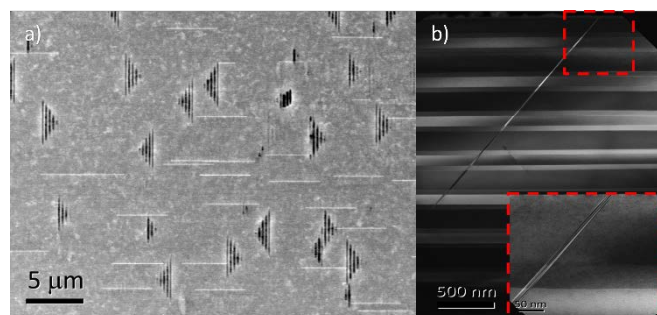


Fig. 1 a)ECCI showing stacking faults and twins in an arrow-like shape b) Dark field  $g = 002$  image showing a planar defect go through all the layers to the surface.

- [1] P. D. Hodgson, M. Hayne, A. J. Robson, Q. D. Zhuang, and L. Danos, “GaSb quantum rings in GaAs/Al<sub>x</sub>Ga<sub>1-x</sub>As quantum wells,” *J. Appl. Phys.*, vol. 119, no. 4, 2016, doi: 10.1063/1.4940880.
- [2] H. Kriaa, A. Guitton, and N. Maloufi, “Fundamental and experimental aspects of diffraction for characterizing dislocations by electron channeling contrast imaging in scanning electron microscope,” *Sci. Rep.*, vol. 7, no. 1, pp. 1–8, 2017, doi: 10.1038/s41598-017-09756-3.

# P11: Optical simulations using a 14-band $\mathbf{k}\cdot\mathbf{p}$ model for infrared detectors based on InAs/InAsSb

<sup>1\*</sup>Zanon, J., <sup>2, 1</sup> Flatté, M. E.

\*lead presenter

<sup>1</sup>j.zanon@tue.nl, Department of Applied Physics and Science Education, Eindhoven University of Technology, Eindhoven 5612 AZ, The Netherlands

<sup>2</sup> Department of Physics and Astronomy, University of Iowa, Iowa City, Iowa 52242, USA

Infrared photodetectors are widely recognized for their different fields of applications, such as in aerospace and medicine technologies. Sb-based photodetectors has drawn particular attention with the possibility of constructing type-II superlattices, which could improve the range in the infrared that the photodetectors nowadays work. As any other device, to achieve the required superlattice design, it is deeply important to have reliable simulations to compare with measurements. Therefore, in this work we present a detailed set of optical simulations using the CADtronics software for three InAs/InAsSb superlattice with different InAs/InAsSb period thicknesses. Commercialized by QuantCAD the CADtronics has a 14-band  $\mathbf{k}\cdot\mathbf{p}$  model [1], which we use in this work to obtain photoluminescence and the change in the index refraction at various temperatures. Our calculations showed that, increasing the period thickness of InAs/InAsSb the photoluminescence peak shifts towards higher energies, i.e., indicating an increase in the superlattice band-gap. From the change in the index refraction, we found four different peaks related with transitions from conduction to valence subband energies. Our results were compared with reported experimental measurements, showing a very good agreement.

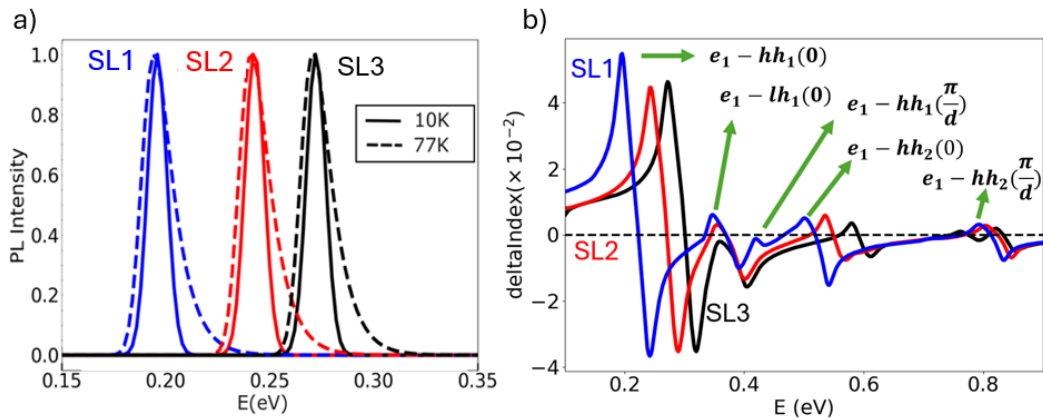


Figure.1. a) shows the normalized photoluminescence (PL) curves, for superlattices (SL) 1, 2 and 3. The index refraction in b) gives the transitions between conduction and valence subbands;  $e$ ,  $hh$  and  $lh$  refer to electron, heavy and light-hole subbands

[1] Lau, Wayne H., J. T. Olesberg, and Michael E. Flatté. "Electronic structures and electron spin decoherence in (001)-grown layered zincblende semiconductors." arXiv preprint cond-mat/0406201 (2004).

This project has received funding from the European Union's Horizon 2020 research and innovation programme under the MarieSkłodowska-Curie grant agreement No 956548.

# P12: Advanced GaSb Quantum Ring LEDs with Distributed Bragg Transmitter for Telecom Wavelength Applications

<sup>1\*</sup>Acar, G., <sup>1</sup>Jones, S., <sup>1</sup>Peter Hodgson, <sup>2</sup>Cesar, F. A., <sup>2</sup>Beanland, R., & <sup>1</sup>Hayne, M.  
<sup>1</sup>Department of Physics, Lancaster University, Lancaster LA1 4YB, UK  
<sup>2</sup>Department of Physics, University of Warwick, Coventry CV4 7AL, UK  
 \*corresponding author: [g.acar@lancaster.ac.uk](mailto:g.acar@lancaster.ac.uk)

In the rapidly advancing field of quantum optoelectronics, achieving single-photon emission at telecommunication wavelengths stands as a fundamental requirement to push the boundaries of photonic quantum computing and enhance the security of quantum cryptography. These technologies require efficient and reliable single photon sources for progress [1].

This study investigates the potential of type-II GaSb quantum rings (QRs) which were produced using the Stranski-Krastanow method by molecular beam epitaxy, as future candidates for electrically driven, ambient-temperature single-photon light-emitting diodes (SPLEDs) that can be mass-produced at low costs [2,3,4]. GaSb QRs offer several advantages over traditional quantum dots, including reduced net stress, fewer defects [5] and a deep hole confining potential suitable for operation at telecommunication wavelengths [2]. We aimed to compare the performance of a standard p-i-n LED with GaSb QRs with that of a novel LED design employing a Distributed Bragg Transmitter (DBT) for enhanced light extraction and transmission. This strategy significantly amplifies the extraction efficiency and narrows the transmission band, aligning with the operational principles of SPLEDs.

After MBE growth, the real layer thicknesses of the DBT LED were measured by transmission electron microscopy. Subsequently, both GaSb QR LED and GaSb QR DBT LED devices were fabricated. Our results show that the DBT LED not only produces brighter electroluminescence peaks than regular LEDs but also matches well with transmission, as well as theoretical prediction, as shown in Fig. 1. a. This confirms the effectiveness of the DBT design. A significant correlation was observed between the results, as shown in Fig. 1. b. The introduction of DBT-enhanced GaSb QR LED represents a pivotal advancement in quantum optoelectronics, showing promising potential for applications in vertical-cavity surface-emitting lasers and SPLEDs, which are crucial in quantum information technology and optical sciences. Our results highlight the essential role of type-II QR devices in improving the device performance for next-generation optical and quantum technologies.

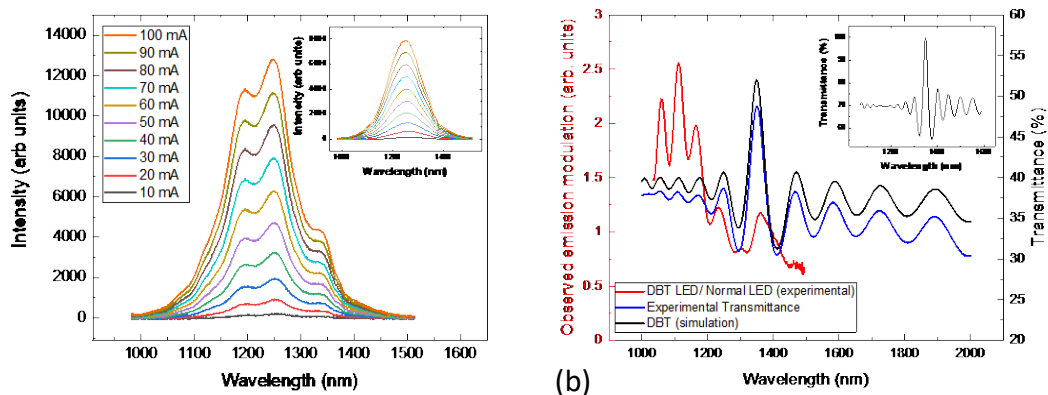


Figure 1. (a) Electroluminescence intensity vs. wavelength for DBT QR LED (main) and normal QR LED (inset). (b) Comparison of simulated (black) and experimental DBT transmission (blue). The red line is the DBT LED emission normalized by normal LED emission.

Acknowledgement: This work is supported by European Union's Horizon 2020 research and innovation programme under the Marie Skłodowska-Curie grant agreement n° 956548, project Quantimomy.

[1] C. Y. Lu *et al*, Nat. Nanotechnol., **16**, 1924-2926 (2021). [2] P. D. Hodgson *et al*, Applied Physics Letter, **105**, 8 (2014).

[3] P. D. Hodgson *et al*, Journal of Applied Physics, **119**, 4 (2016).

[4] M. Hayne *et al*, *Single photon source*, patent application, WO2018162894A1 (2018).

[5] R. Timm *et al*. J. Vac. Sci. Technol. B **26**, 1492- 1492-1503, (2008).

# P13: GaAsGe ternary alloys studied by cross-sectional scanning tunneling microscopy

<sup>1\*</sup>Trevisan A., <sup>1</sup>van Lierop W., <sup>2</sup>Ripalda J. M., <sup>2</sup>González Y., <sup>2</sup>Caño P., <sup>2</sup>Navarro E., <sup>3</sup>Juluri R., <sup>3</sup>Sanchez A. M. & <sup>1</sup>Koenraad P. M.

\*lead presenter

<sup>1</sup>a.trevisan@tue.nl, Department of Applied Physics and Science Educations, Eindhoven University of Technology, The Netherlands

<sup>2</sup> Instituto de Microelectrónica de Madrid, Spanish National Research Council (CSIC), Spain

<sup>3</sup> Department of Physics, University of Warwick, Coventry, United Kingdom

Similarly to Si, Ge exhibit an amphoteric behavior when used as dopant in GaAs, i.e. it can substitute both Ga and As atoms.<sup>[1]</sup> In molecular beam epitaxy grown GaAsGe, at low doping concentration Ge preferentially substitute either Ga or As atoms depending on the growth condition, namely the As<sub>2</sub> to Ga ratio in the molecular beams.<sup>[2]</sup> However, at high doping concentration, Ge is expected to substitute Ga and As atom to the same extent.<sup>[1],[3]</sup>

A GaAs/GaAs:Ge structure comprising of seven 50 nm-thick GaAs:Ge layers with decreasing Ge concentration (5%, 3%, 1%, 0.5%, 0.1%, 0.05% and 0.01% Ge) grown by molecular beam epitaxy was analyzed by cross-sectional scanning tunneling microscopy (X-STM). All the layers aside the 5% Ge one were imaged by X-STM. In filled-states X-STM images, the Ge atoms appear as bright features (Fig. 1) with different shapes depending on where they are located in the GaAs lattice, namely whether they are sitting on a Ga or As site and at what depth below the cleaved surface (0<sup>th</sup> layer).

Several features are identified in the layer at lower Ge concentration, i.e. 0.01% Ge (L7). Of these features we assume that some correspond to a Ge atom sitting on a Ga-site located at different depth below the cleaved surface. Similarly, some other features are related Ge atoms on As-sites located at different depth below the surface. These different features have been classified and related to the Ge position below the cleaved surface through symmetry considerations taking into account the contribution of the different surface states to the X-STM images, i.e. the A<sub>4</sub> and A<sub>5</sub> state located in the valence band and the C<sub>3</sub> and C<sub>4</sub> located in the conduction band. Other observed features are given by Ge located deeper below the cleaved surface (5<sup>th</sup> layer or lower) and vacancies that can be either intrinsic or caused by the cleave of the sample.

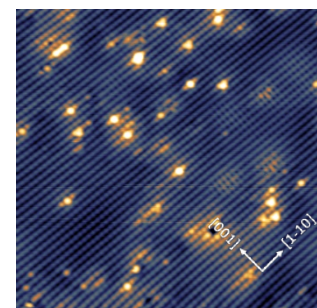
Additionally, we calculated the Ge concentration in the measured layers and we compared it to the nominal concentration. We found that for most the layers, the experimental concentration is comparable to the nominal one.

With this study, we aim to gain further insight into the preferential incorporation of Ge in GaAs, which is difficult to determine with other techniques.

## References

- <sup>[1]</sup> C. M. Wolfe, G. E. Stillman, *Appl. Phys. Lett.* 27, 564–567 (1975)
- <sup>[2]</sup> A. Y. Cho and L. Hayashi, *J. Appl. Phys.* 42, 4422–4425 (1971)
- <sup>[3]</sup> R. J. Baird *et al.*, *J. Appl. Phys.* 69, 226–236 (1991)
- <sup>[4]</sup> Ph. Ebert, *Surf. Sci. Rep.* 33, 121–303 (1999)
- <sup>[5]</sup> D. Tjeertes *et al.*, *Phys. Rev. B.* 104, 125433 (2021)

Fig. 1. 25.0 × 25.0 nm<sup>2</sup> X-STM image of GaAsGe (0.5% Ge), V<sub>b</sub> = -3.24 V, I<sub>t</sub> = 50 pA, 77K.



# P14: Simulations of the triple-barrier resonant-tunnelling heterostructure for ULTRARAM memory

<sup>1</sup>\*Xiuxin Xia, <sup>1,2</sup>Peter D. Hodgson, <sup>1,2</sup>Manus Hayne.

\*lead presenter

<sup>1</sup>x.xia7@lancaster.ac.uk, Lancaster University, UK

<sup>2</sup>Quinas Technology Limited, UK

DRAM and flash prevail in computer memories, serving as main memory and data storage respectively, with their complementary characteristics providing a balance of speed, non-volatility and cost. Built from a transistor-capacitor (1T-1C) structure, DRAM requires periodic refreshing and thus suffers data loss when power is off. To the contrary, flash holds charges via a thick oxide layer hence no power supply is needed for retaining the data. However, it needs a larger voltage and longer time to change the binary value than DRAM, so has poor program/erase performance and catastrophic wear occurs after a relatively low number of program/erase cycles, i.e., it has poor endurance. Given this context, a ‘universal memory’ that delivers the speed, endurance and other advantages of DRAM as well as the non-volatility of flash has been considered to be paradox.

**ULTRARAM**, a III-V compound semiconductor memory, tackles the dilemma by employing a triple-barrier resonant-tunnelling structure (TBRT) to replace the oxide found in the conventional flash structure. The band offsets between InAs and AlSb in the TBRT keep the charges trapped in the floating gate until it becomes electrically transparent when appropriate bias is applied. Therefore, **ULTRARAM** offers non-volatility as well as speed. The TBRT allows orders of magnitude lower switching energies to be achieved compared to other memory technologies [1]. Simulations of the TBRT have shown that it is robust against layer thickness variations, which can happen during sample growth [2], indicating great potential for the volume production. Compatibility with semiconductor manufacturing was validated by experiential verification of **ULTRARAM** with a gate dimension of 10  $\mu\text{m}$  on Si substrate [3].

Previous simulation work focused on the layer variation which can happen during molecular beam epitaxy (MBE) as the thinnest TBRT barrier layer contains only two monolayers. However, studies using cross-sectional imaging by electron microscopy have revealed that interface alloying is an additional issue. Simulations using nextnano [4] concerning interface alloying of several variations in the TBRT heterostructure are discussed and presented. Results shows that alloying in the InAs quantum well is more detrimental than in barrier which only pushes the tunnelling voltage to higher level, however none of the alloying cases simulated to date undermine the concept of TBRT operation.

**Acknowledgement:** This work is supported by European Union’s Horizon 2020 research and innovation programme under the Marie Skłodowska-Curie grant agreement n° 956548, project Quantimony.

[1] Tizno, Ofogh, *et al.* Scientific reports 9.1 (2019): 1-8. [2] Lane, Dominic, and Hayne, Manus, *Journal of Physics D: Applied Physics* 54.35 (2021): 355104. [3] Hodgson, Peter D., *et al.* *Advanced Electronic Materials* (2022): 2101103. [4] S. Birner, Website of nextnano GmbH company, available at: <https://www.nextnano.com/>

# P15: A k·p interface model for InAs/GaSb Type-II superlattices simulation by nextnano<sup>3</sup>

Chen Liu<sup>1,2\*</sup>, Anh-Luan Phan<sup>3</sup>, Takuma Sato<sup>4</sup>, Julian Zanon<sup>5</sup>, Manoj Kesaria<sup>1</sup>, Iwan Davies<sup>2</sup>

\*Email: [chenliu@iqep.com](mailto:chenliu@iqep.com)

<sup>1</sup>School of Physics and Astronomy, Cardiff University, United Kingdom

<sup>2</sup>IQE plc, Cardiff, Wales, CF3 0LW, United Kingdom

<sup>3</sup>Department of Electronics Engineering, University of Rome Tor Vergata, Rome, Italy

<sup>4</sup>nextnano GmbH, Munich, Bavaria, Germany

<sup>5</sup>Applied Physics and Science Education, Eindhoven University of Technology, Eindhoven, Netherlands

Mid-wave and long-wave infrared detectors are crucial in various applications, including night vision, motion detection, and thermal imaging [1]. InAs/GaSb Type-II superlattices (T2SLs) have emerged as promising alternatives to HgCdTe for infrared detectors [2] due to their flexible band gap engineering and advantageous manufacturability. However, designing a detector based on InAs/GaSb T2SLs requires careful consideration of the layer thickness, which are crucial for tuning the growth conditions. Despite excellent achievements in experiments [3], the increasing demand for simulation tools in device design is evident.

Here we present an approach based on the 8-band k·p method within the framework of nextnano<sup>3</sup> for calculating the band gaps of InAs/GaSb T2SLs. An interface Hamiltonian was applied at the interfaces between InAs and GaSb layers [4]. Our approach effectively predicts the band gaps of various InAs/GaSb T2SLs with InSb interfaces grown on GaSb substrates across short-wave to long-wave range (Fig.1 (a)). Besides, it can forecast the spectral blueshift (Fig.1 (b)) and redshift (Fig.1 (c)) of band gaps for InAs/GaSb T2SLs with increasing GaSb and InAs sublayer thicknesses, respectively.

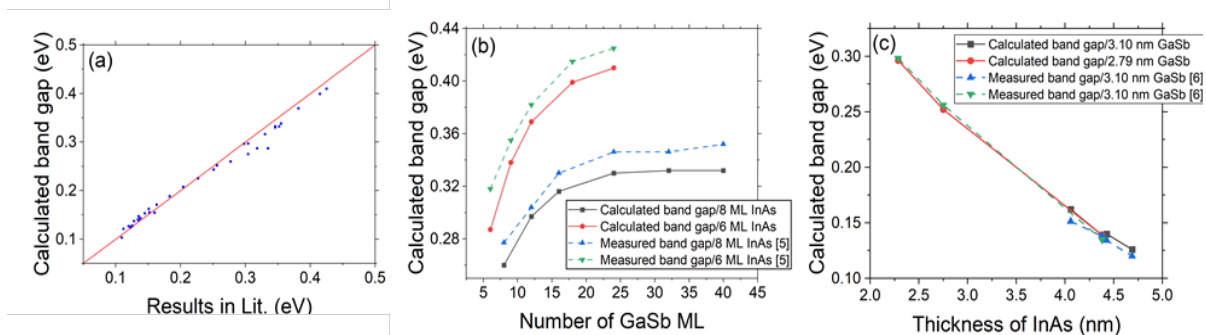
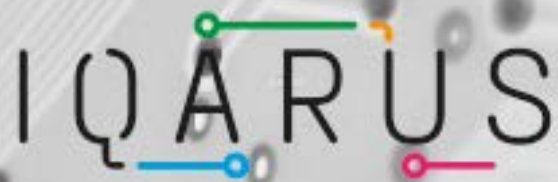


**Fig.1** (a) Comparison between calculated band gaps and results in literature for various InAs/GaSb T2SLs. (b) Spectral blueshift of band gaps with increasing GaSb thickness at fixed InAs thickness. (c) Spectral redshift of band gaps with increasing InAs thickness at fixed GaSb thickness

## References:

- [1] F. Zhuge et al., *Adv. Mater. Technol.* 2, 1700005 (2017). [2] A. Rogalski, *Infrared Phys. Technol.* 54, 136-1545 (2011). [3] D. C. M. Kwan et al., *Appl. Phys. Lett.* 118, 203102 (2021). [4] P. C. Klipstein et al., *Infrared. Phys. Technol.* 59, 53-59 (2013). [5] A. Ongstad et al., *J. Appl. Phys.* 89, 2185 (2001). [6] R. Rehm et al., *Infrared. Phys. Technol.* 59, 6-11 (2013).



# IQARUS

International Workshop on Quantum  
Antimonides Research & Upscaling

## BOOK OF ABSTRACTS

[www.iqarus.org](http://www.iqarus.org)